Renewable and Sustainable Energy Reviews 55 (2016) 823–839

Contents lists available at ScienceDirect

Renewable and Sustainable Energy Reviews

journal homepage: www.elsevier.com/locate/rser

A comprehensive review of low-voltage-ride-through methods for fixed-speed wind power generators

Amirhasan Moghadasi [a,b,*], Arif Sarwat [a,b], Josep M. Guerrero [c]

[a] Energy Systems Research Laboratory, Florida International University, FL 3920, FL, USA
[b] Electrical and Computer Engineering Department, Florida International University (FIU), FL, USA
[c] Department of Energy Technology, Aalborg University, Aalborg, Denmark

ARTICLE INFO

Article history:
Received 7 February 2015
Received in revised form
6 September 2015
Accepted 12 November 2015
Available online 5 December 2015

Keywords:
Economic feasibility
Fixed-speed induction generators (FSIGs)
Low voltage ride-through (LVRT)
Wind turbines (WTs)

ABSTRACT

This paper presents a comprehensive review of various techniques employed to enhance the low voltage ride through (LVRT) capability of the fixed-speed induction generators (FSIGs)-based wind turbines (WTs), which has a non-negligible 20% contribution of the existing wind energy in the world. As the FSIG-based WT system is directly connected to the grid with no power electronic interfaces, terminal voltage or reactive power output may not be precisely controlled. Thus, various LVRT strategies based on installation of the additional supporting technologies have been proposed in the literature. Although the various individual technologies are well documented, a comparative study of existing approaches has not been reported so far. This paper attempts to fill this void by providing a comprehensive analysis of these LVRT methods for FSIG-based WTs in terms of dynamic performance, controller complexity, and economic feasibility. A novel feature of this paper is to categorize LVRT capability enhancement approaches into three main groups depending on the connection configuration: series, shunt, and series–shunt (hybrid) connections and then discuss their advantages and limitations in detail. For verification purposes, several simulations are presented in MATLAB software to demonstrate and compare the reviewed LVRT schemes. Based on the simulated results, series connection dynamic voltage restorer (DVR) and shunt connection static synchronous compensators (STATCOM) are the highly efficient LVRT capability enhancement approaches.

Contents

* Correspondence to: Florida International University (FIU), 10555 West Flagler Street, EC 3913 Miami, FL 33174, USA. Tel.: +1 305 348 2935 (Lab).
E-mail address: amogh004@fiu.edu (A. Moghadasi).

http://dx.doi.org/10.1016/j.rser.2015.11.020
1364-0321/

1. Introduction

Fortunately, the goal of reducing green-house gas emissions is aligned, to a significant extent, with the evolution and penetration of renewable energy sources (RES) [1]. The attempts to reduce the continued pollution are promising in view of the recent dramatic increase of installed wind turbines' (WTs) capacity [2–4]. However, grid integration of large WTs can pose serious adverse effects in weak or faulty grids [5]. The trend towards the integration of more WTs contributes to the increase in the fault current levels, as well as voltage reductions at the terminals of wind generators, which may lead to the disconnection of WTs, and consequently affects power system stability during and after fault clearance [6–8].

Recently, many power system operators in Europe and other regions of the world have begun expanding and modifying their interconnection requirements for wind farms through technical standards, known as grid codes [9,10]. One of the critical requirements concerning the grid voltage support is the low voltage ride-through (LVRT) capability, which is included in many new grid codes [11–15]. Fig. 1(a) shows a practical example of the LVRT curve defined by the Danish system operator (Energinet.dk) for WTs connected to the grid [16]. Based on this regulation, if the voltage remains at a level greater than 20% of nominal value for a period of less than 0.5 s, the WT should remain connected to the grid.

WTs are only allowed to disconnect from the grid when the voltage profile falls into Area B. Besides the LVRT requirements, some grid codes require large WTs to contribute to the voltage restoration of the power system by injecting the reactive power during the fault and the recovery period [17,18], while maintaining the operating point above the area of Fig. 1(b). A literature review on international grid codes for wind power integration has been discussed and summarized in [19–23].

Although most wind turbine generators manufactured today are doubly-fed induction generators (DFIGs) [24,25] and permanent-magnet synchronous generators (PMSGs) [26], a non-negligible 20% of the existing wind energy in Europe is still employing fixed-speed induction generators (FSIGs) due to their simple structure and lower maintenance cost [27,28]. Thus, the fault-ride through characteristics of FSIG-based wind turbines still need to be analyzed. However, this technology is unable to fulfill new grid code requirements since they have no power electronic converters to control terminal voltage and reactive power output. In this case, induction generators may suffer from a voltage instability problem, which is becoming a significant concern with large-scale wind farm penetration. Therefore, technical solutions must be developed in order to ensure that those wind farms fulfill grid code requirements for their operations.

In the recent literature, various studies have been individually documented in terms of installing additional supporting technologies to enhance the LVRT capability of the FSIGs-based WTs, which need to be properly reviewed and discussed.

Although there are a few valuable review papers of LVRT enhancement strategies for DFIGs and PMSGs-based WTs [29–31], up to the present time, as far as the authors are aware, there has been no comprehensive report, fully considering LVRT improvement methods of FSIGs based WTs. Ref. [32] only presented a brief review and comparison of the series compensators for LVRT enhancement of a wind generator system based on FSIGs.

The main contributions of this paper are organized into the following sections: after describing the operation of the FSIG-based WT under normal and faulty conditions in Section 2, the comprehensive review of the recently LVRT capability improvement approaches is discussed in Section 3. The reviewed methodologies are classified into the three main groups, namely, (i) series-connected solutions (i.e., thyristor-controlled series compensation (TCSC), dynamic voltage restore (DVR), series dynamic braking resistor (SDBR), magnetic energy recovery switch (MERS), and fault current limiter (FCL)); (ii) shunt-connected solutions (i.e., static var compensator (SVC), static synchronous compensator

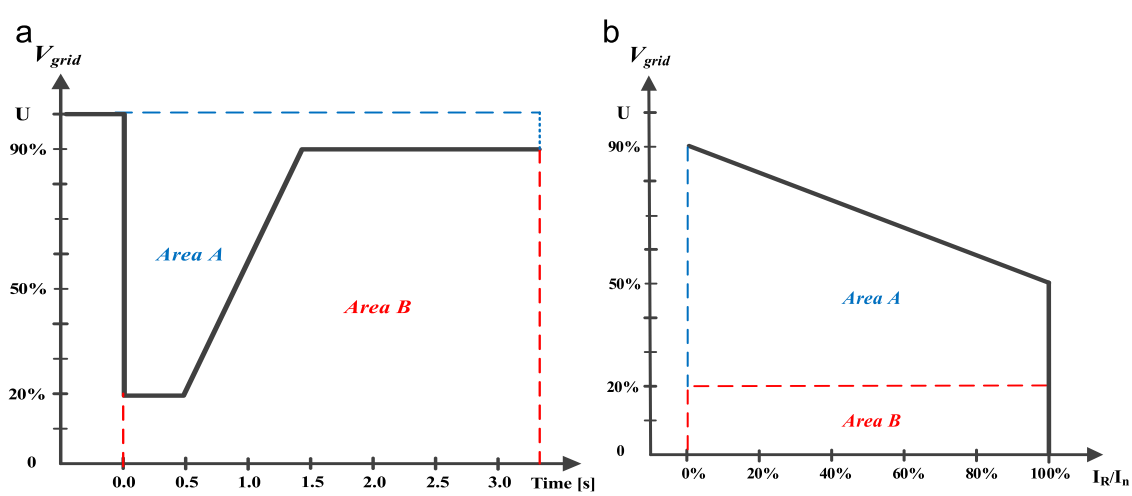

Fig. 1. Danish grid codes. (a) LVRT requirement. (b) Reactive power support requirement.

(STATCOM), and superconducting dynamic synchronous condenser (SDSC)); (iii) hybrid-connected solutions (i.e., unified power quality conditioner (UPQC), and unified compensation system (UCS)). A comparative study in terms of dynamic performance, controller complexity, and cost evaluation of these LVRT methods is carried out in Section 4. In Section 5, simulation results of several LVRT methods are illustrated to compare the dynamic performance of the wind turbine equipped with auxiliary devices. Finally, the conclusions are presented in Section 6.

2. FSIG-based wind turbine

A non-negligible number of WTs equipped with induction generators are still in operation at an almost fixed speed due to wide usage of early wind turbine systems. These were the first Danish wind turbines which completely dominated the market up to the mid-1990s, hence the reason why this technology is named Danish concept [28,33,34]. The basic configuration of the WT based on FSIG is shown in Fig. 2, including a turbine rotor, gearbox, squirrel-cage induction generator, soft-starter, mechanical-switched capacitors (MSCs), and a transformer for grid connection.

2.1. Steady-state operation

WTs extract the power from the wind via aerodynamically designed blades and convert it to mechanical power. Under high wind speed conditions, the power delivered by a WT may exceed its rated value. Thus, an effective approach must be applied to reduce a portion of the wind power so as to avoid turbine damages. The aerodynamics of fixed-speed wind turbines can be controlled by *passive stall*, *active-stall*, and *pitch control* approaches which have been developed for low, medium, and large WTs, respectively [35,36]. An example of the relationship between the wind speed and the power generated by the wind turbine is shown in Fig. 3 [37]. The blades start to move around 4 m/s, and optimal aerodynamic efficiency is achieved at the wind speed rated about 15 m/s. The extra power obtained from wind speed between 15 and 25 m/s may be smoothly curtailed by spinning the blades using either active stall or pitch control to avoid overloading the wind turbine system. Over the cutout wind speed, the turbine has to be disconnected in order to avoid damage. It has been reported that the pitch control has become dominant in the wind power market (used four times more than the stall control) [38].

Many methods of WT pitch control have been documented such as the classical proportional-integral-derivative (PID) control [39], gain-scheduling control [40], or robust control [41], among other nonlinear controllers [42]. Fig. 4 depicts the conventional pitch angle regulator in which the input and output of the model are the generated power P_{out} and blade angle β, respectively. The gearbox plays an essential role in the fixed speed WTs to adapt low-speed, high-torque rotation of the turbine rotor into the faster rotation of the electrical generator [38]. The critical issue in implementing the gearbox technology is the wind gusts and turbulences, which may lead to misalignment of the drive train and a gradual failure of the gear components, consequently increasing the capital and operating cost of the WTs [43].

Induction generators with squirrel-cage rotor can be used in the fixed-speed WTs at low cost and with low maintenance due to rugged brushless construction [28,33,44]. Nevertheless, it has some important drawbacks, as it requires a stiff power grid to enable stable operation, and may also require a more expensive mechanical construction in order to absorb high mechanical stress, since wind gusts can cause torque pulsations on the drive train [37]. Moreover, the induction generators tend to draw large amount of reactive power from the grid in their steady-state operation for self-excitation because stator windings are directly connected to the grid with no power electronics [45]. Thus, the low-cost MSCs generally includes a bank of shunt capacitors are connected to the terminal of the wind generator to achieve a unit power factor and provide voltage regulation in normal operation conditions [46].

The high starting inrush currents generated by the connection of induction generators to the power system may cause disturbances to both the grid voltage and high torque spikes in the drive train of WTs. Thus, current limiters or soft-starters based on thyristor technology are used to typically limit the rms value of the inrush currents to a level below two times of the generator rated current [37]. Further, the soft-starters effectively dampen the torque peaks associated with the peak currents, and hence reduce the loads on the gearbox.

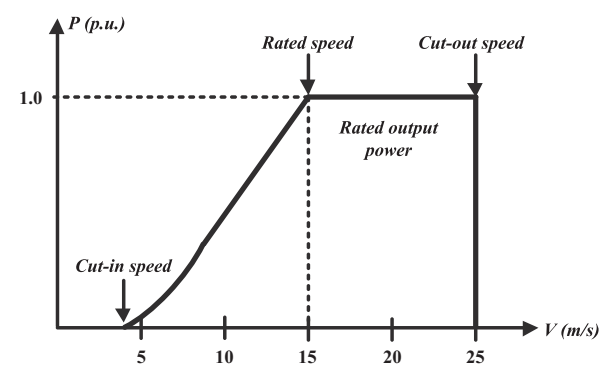

Fig. 3. The output power of a wind turbine as a function of the wind speed [37].

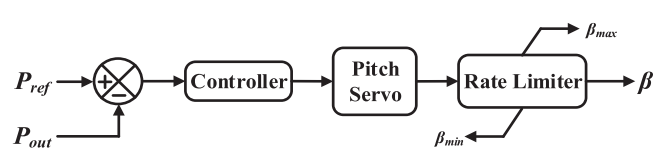

Fig. 4. Conventional pitch angle control used in FSIG-based wind turbine.

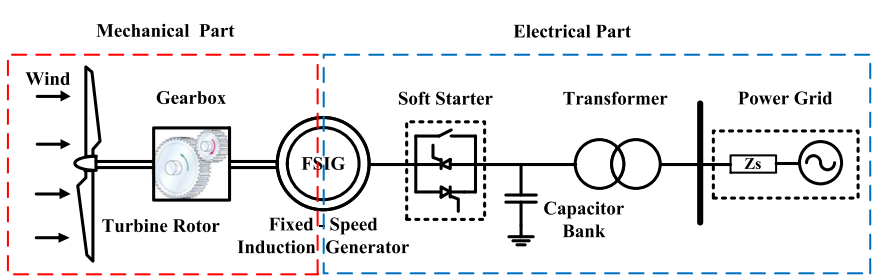

Fig. 2. The main components of the wind turbine based on FSIG.

2.2. Transient-state operation

When the fault starts, the voltage at the terminals of the WT drops down, thus leading to significant reduction in electromagnetic torque and electric-power output of the induction generator. However, the mechanical-input torque remains constant during the fault, causing the rotor speed increases beyond its safety limits in order to mechanically store the energy excess [47]. Therefore, it is important to keep the balance between the mechanical-input power and the electrical-output power for enhancing the fault ride-through capability of FSIG-based WT.

After the fault clearance, since the rotor speed increases during the fault period, a large amount of reactive power is absorbed by induction generator from the grid. As a consequence, not only induction generator is not able to fulfill the reactive injection requirements along the fault, but also it exacerbates the voltage sag condition by absorbing reactive power, making it difficult to restore the terminal voltage within the acceptable level [19]. As illustrated in Fig. 4, if P_{out} exceeds its rated value, the pitch angle β increase to limit generated wind power to its rated value. Under fault conditions, the generated power is abruptly falls and it is unable to perfectly contribute in LVRT improvement.

To overcome this drawbacks, the modified pitch angle controllers are proposed in the literature based on wind generator speed, so that these can immediately increase the pitch angle to reduce the mechanical-input torque, as shown in Fig. 5 [48–50]. Although pitch control system is the cheapest solution for enhancing the LVRT capability of FSIG-based wind turbine, but it has very slow dynamic response due to the mechanical constraints of the system [51].

Also, MSCs represent relatively weak performance during fault conditions, owing to the decrease of their reactive power injection capability following voltage drops. Furthermore, excessive switching of the capacitor bank provokes failures, applies the inherent voltage steps stress on the wind turbines, and increases the required maintenance of the system [37].

The above discussions have covered symmetrical grid faults, but in general the majority of grid faults result in asymmetrical voltage dips with both positive and negative sequence components. When the grid voltage is unbalanced, i.e. it contains a fundamental negative sequence component, the stator current of induction generator becomes unbalanced as well. As stated in [52], a slight amount of negative-sequence voltage causes higher amounts of negative-sequence currents, and consequently creates the additional torque oscillations of the double grid frequency, resulting in heating of the stator windings, thus reducing the life span of the gearbox, blade assembly, and other components of a typical WT [53–55]. The magnitude of the negative and positive sequences of the torque can be calculated as follows [56]:

$$T^{+} \cong 3 \times \frac{p}{2\omega_s} \times V_s^{+} \times I_s^{+} \tag{1}$$

$$T^{-} \cong 3 \times \frac{p}{2\omega_s} \times V_s^{+} \times I_s^{-} \tag{2}$$

where T^{+} and T^{-} are the positive and negative torque sequences, p is the number of poles, ω_s is the sliding angular frequency, $V_s{}^{+}$ is positive-sequence voltage, $I_s{}^{+}$ and I_s^{-} are positive and negative current sequences, respectively. It is clear from (1) and (2) that the average torque is reduced due to the decreased positive-sequence voltage, leading to the acceleration of the induction generator, mechanical vibrations, and acoustic noise. The response of WTs based on FSIG during asymmetrical faults have been investigated in the literature and several control methods injecting negative sequence current have been proposed to balance the grid voltage by reducing the negative sequence voltage [55–59].

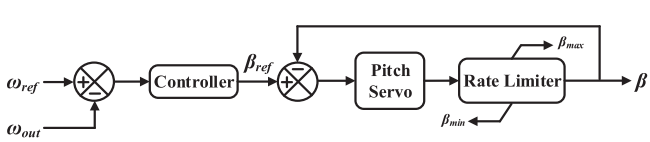

Fig. 5. Modified pitch angle control used in FSIG-based wind turbine.

3. Low voltage ride-through strategies for FSIG-based WTs

As discussed previously, the LVRT performance of FSIG-based wind turbines is problematic because the stator windings are directly coupled to the grid, and the induction generator consumes reactive power during and after a fault. Therefore, it fails to fulfill some of the important grid integration requirements, such as reactive power compensation or terminal voltage control. Thus, the induction generators need the external supporting devices to avoid their tripping during voltage reduction.

There are many auxiliary devices reported in the literature to provide adequate dynamic voltage support and enhance the LVRT capability of WTs. The major categories of LVRT methods of FSIG-based wind turbine are depicted in Fig. 6. Depending on the connection configuration, these methods can be classified into the series-connected solutions [60–102], shunt-connected solutions [103–127], and hybrid-connected solutions [128–132].

3.1. Review of series-connected solutions

Series-connected auxiliary technologies have been successfully implemented to alleviate grid congestion, defer construction of new transmission lines, and improve system capacity. These types of technologies, as a relatively simple solution, with a smaller current injection compared to shunt-connected technologies, is effectively used to regulate voltage or limit fault current resulting significant increase in the transient and voltage stability in transmission systems. A brief explanation of series-connected solutions is presented in the following subsections.

3.1.1. Thyristor-controlled series compensation (TCSC)

The essential principle of the TCSC is to control power flow of the grid lines, increase the dynamic stability of power transmission, and effectively limit the power oscillations [60–62]. These features have been effectively proven by existing installations of TCSCs described in the literature, such as the Western Area Power Administration's Kayenta site [63], or the Bonneville Power Administration's Slatt substation [64]. Recently, the abilities of this technology have particularly been realized where inconstancy in the transmission lines for delivering the huge WT generated power into the grid, lead to voltage collapse and cut off the fixed speed WT [65,66]. Moreover, the ability of TCSC to limit fault current and control voltage unbalance of wind farm systems is discussed in [67]. Fig. 7 illustrates a typical TCSC module installed outside the wind farm along with the basic control scheme. A TCSC consists of three components: capacitor banks C, bypass inductor L, and forward-biased thyristors T_1 and T_2. The control scheme has been well-documented in the literature [60,61]. The function of

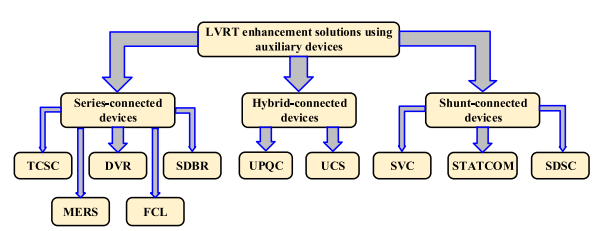

Fig. 6. Classified LVRT capability enhancement methods.

the control block is to generate appropriate gate drive signals for the thyristors when the fault is initiated. Basically, thyristors are fired with respect to zero crossing of the line current to inject additional current into the capacitor through the bypass inductor and increase the capacitive reactance value, typically up to a factor of three times the original reactance. This way, a variable capacitive reactance can be obtained to compensate the reactive power absorbed by the induction generator, improve the fault right through of WT. This technology may be useful for wind farms located far away from the PCC, such as offshore wind farms [37].

3.1.2. Dynamic voltage restorer (DVR)

A promising approach to effectively overcome the grid-fault-derived problems with WT generators and to enhance ride-through capability is to control the connection-point voltage by compensating voltage fluctuations during the fault. This can be accomplished by using a series-connected power electronic compensator called dynamic voltage restorer (DVR) which injects an appropriate voltage into the grid bus to keep the generator voltage constant at PCC and with the same phase as the network, as shown in Fig. 8. Depending on the time frame assumed by the regional grid code (e.g. in the Danish electrical system 80% three-phase voltage-dips should be ride-through for up to 30 grid-cycles), a DVR might have a sufficient energy storage capacity to generate missing voltage at the WT terminal during the dips. There are several efforts that demonstrate the utilization of a DVR for voltage dip mitigation and voltage recovery in which DVR restores the WT terminal voltage to the operating point within the shaded area of the LVRT curve [68–70]. Industrial examples of DVRs are also given in [71,72]. However, by using a DVR for voltage sag mitigation in fixed-speed wind generators has certain technical challenges [73]. According to the voltage vector diagram shown in Fig. 9(a), the voltage dip is causing not only a reduction in voltage magnitude, but also a change in phase, which is described as a phase angle jump δ (phase angle difference between the voltage phase during the sag and the one before the sag), which can be obtained as following [74]:

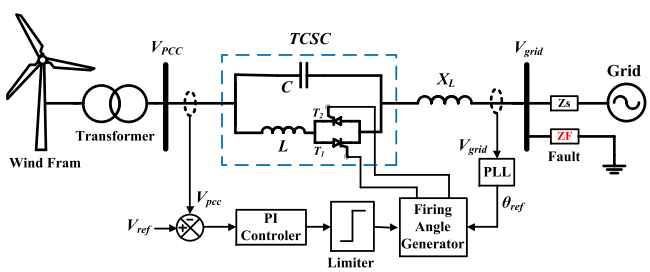

Fig. 7. TCSC module installed outside the wind farm with the basic control scheme.

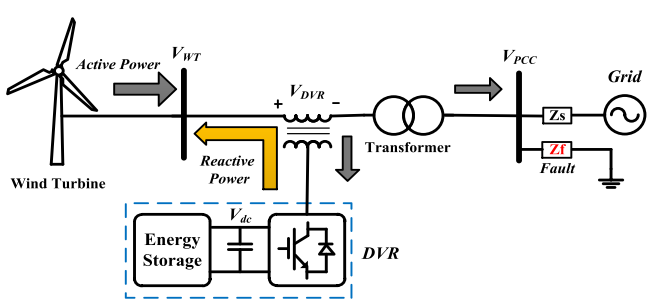

Fig. 8. Principle operation of the dynamic voltage restorer and power flow during the voltage dip compensation.

$$\delta = \arctan\left(\frac{X_F}{R_F}\right) - \arctan\left(\frac{X_s + X_F}{R_s + R_F}\right) \tag{3}$$

where $Zs = Rs + jXs$ and $Z_F = R_F + jX_F$ are gird impedance and fault impedance, respectively.

The phase-angle jump reveals itself as a shift in zero crossing of the instantaneous voltage, causing a large transient at the beginning and the end of the sag because the internal generator flux is out of phase with the voltage [70,75].

Moreover, the DVR requires absorbing part of the extra active power generated by the wind generator during the fault to keep dc-link voltage (V_{dc}) at the desire level, thus it must has energy dissipation capabilities which is the main drawback of the DVR (see Fig. 10). To address the aforementioned problems, some successful control schemes are discussed in the literature [70,76–79]. In the work described in [70], the energy dissipation was accomplished by using a resistor which is connected to the dc link through a power electronic switch, once the dc-link voltage exceeds its safety limits. The decoupled control of d- and q-axis voltages have been reported in [76,78] for the DVR inverter to improve the LVRT capability of the FSIG based WTs. In [79], the authors propose an adaptive control system based on proportional+resonant (PR) controller to provide voltage and current decoupling in order to improve the DVR output voltage tracking capability. In [70], Dionisio et al. carried out a control scheme based on a two-step strategy. First, the DVR compensated the voltage sag to maintain the magnitude and phase of the wind generator voltage at 1 pu and second, control system gradually rotated the series voltage supplied by the DVR, V_{DVR}, in order to inject reactive power into the grid while the magnitude of the wind generator voltage was kept at 1 pu (see Fig. 9(b)).

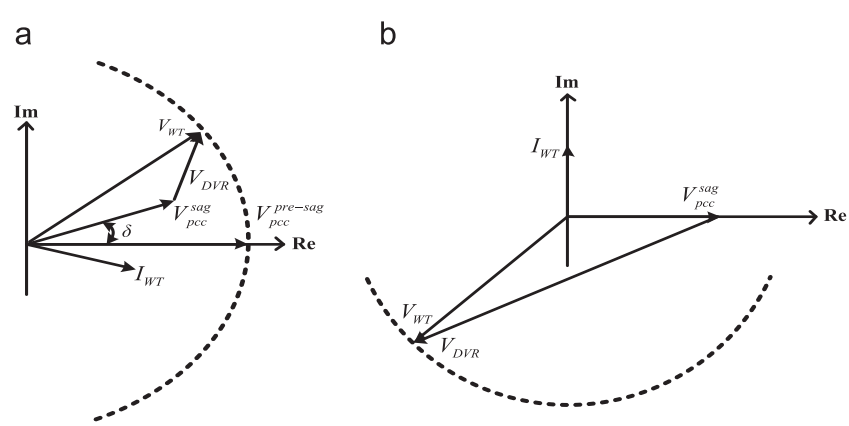

Fig. 9. Single-phase vector diagram. (a) Voltage dip compensation with DVR. (b) Voltage dip compensation once the phasor has been rotated.

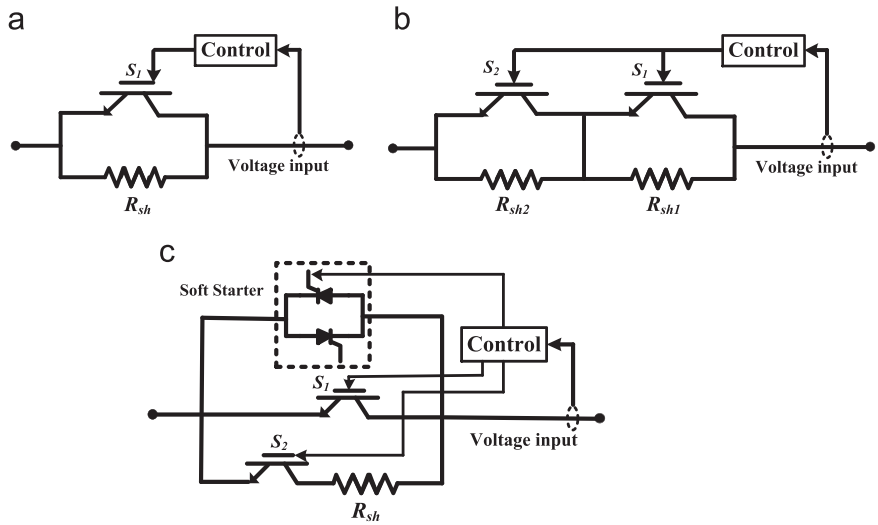

Fig. 10. Various types of SDBR; (a) Single-stage scheme. (b) Two-stage switching scheme. (c) Variable resistor scheme using soft-starter.

3.1.3. Series dynamic braking resistor (SDBR)

The concept of series-connected dynamic braking resistors (series-DBRs) in wind power application was early introduced by the authors in 2004–2005 [80]. DBRs have been developed to contribute directly to the balance of active power between the mechanical and electrical side of the WT system during a fault, potentially reduce or eliminate the need for pitch angle control or reactive power compensation (RPC) devices [81,82]. This is performed by dynamically installing a resistor in series between the WT and the grid, in order to boost the voltage at the terminals of the generator, and thereby alleviate the instability concerns on electrical torque and power during the fault period [83].

The typical schematic layout of SDBR may incorporate one or two stages of resistor/switch units, as shown in Fig. 10(a) and (b), including the static bypass switch, allowing sub-cycle response and smoothly variable control [84]. Under normal conditions, dynamic braking resistor must be cut off by closing the bypass switch. At the beginning of the fault, the current start the passing through the resistor, R_{sh} and continue in operation in the initial post-fault recovery. Once the voltage recovered above a minimum set point level and met the grid code compliance, the bypass switch is closed and the circuit is returned to its normal state. Fig. 10(c) also displays a possible arrangement, using thyristor based soft-starter that is already utilized for a grid connected FSIG-based wind turbine, can enable continuous, optimized control of dynamic braking resistance [84]. Also, ABB represented an additional feature for SDBR scheme, in which the resistors were independently controlled in each of the three phases, enhancing the scheme's performance during unbalanced fault condition [85]. The effect of SDBR on stator voltage is displayed by the phasor diagram of Fig. 11, where the stator voltage is increased across SDBR.

Since the mechanical torque generated by the induction generator changes with the square of the voltage, the presence of SDBR can increase the mechanical power extracted from the drive train therefore, reducing its rotor speed during a voltage dip. This action can also enhance the post-fault recovery of a WT system.

3.1.4. Magnetic energy recovery switch (MERS)

The MERS has recently been proposed as a variable series compensator between the main transformer of the wind farm and power grid to improve the LVRT capability of fixed-speed WTs by compensating the reactive power and controlling the terminal voltage of WT [86–89]. The circuit configuration of the MERS is

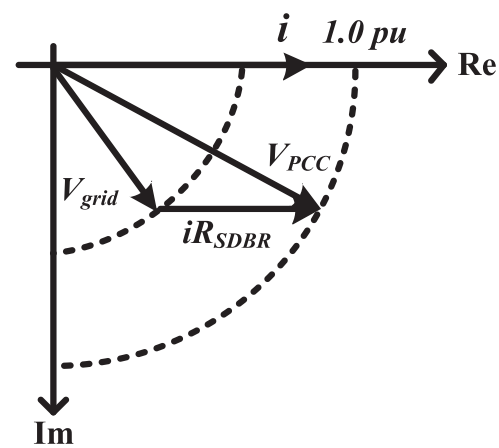

Fig. 11. Single-phase vector diagram for voltage dip compensation with SDBR [81].

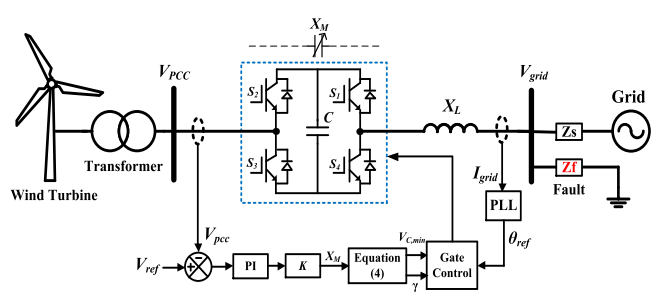

Fig. 12. Circuit configuration of the MERS for controlling the series-injected voltage.

shown in Fig. 12, including four reverse conductive semiconductor switches and a dc capacitor. As it is obvious from Fig. 12, that it has a similar topology with respect to a single-phase full-bridge inverter with the exception that dc-link capacitor is several times smaller than that of a single-phase full bridge inverter, due to the capacitor voltage is permitted to alter considerably and to become zero during each fundamental cycle (50 or 60 Hz) [89]. Moreover, this scheme possesses fewer losses compared to the PWM converters so that semiconductors in MERS are switched synchronously to the line frequency which is extremely important for high-power wind applications. The principal

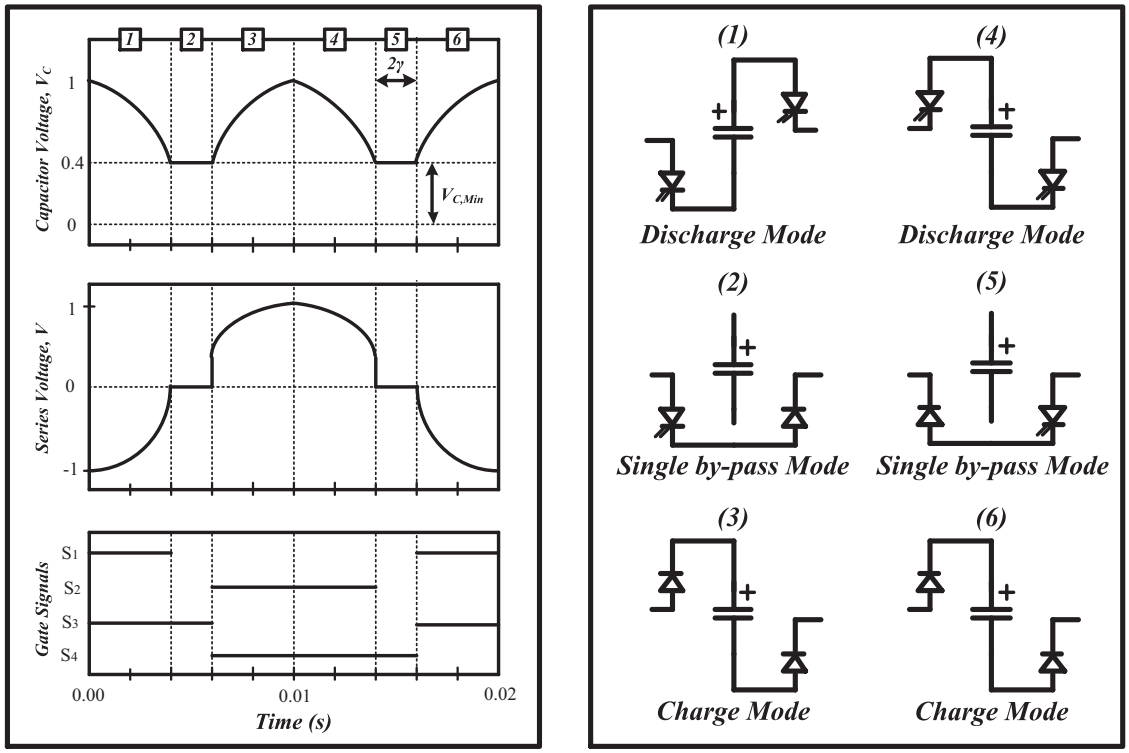

Fig. 13. Switching patterns for one current cycle. (Left part) Voltage and current waveform of MERS. (Right part) The flow of the current through the MERS for the different areas illustrated on the left [89].

results of switching patterns and waveforms for one fundamental cycle are illustrated in Fig. 13 based on two main set-points control, i.e. minimum capacitor voltage, $V_{C,min}$ and the length of the zero injected voltage period, 2γ. By adjusting the $V_{C,min}$ and the γ reference, the current passing through the device can be regulated to provide the variable series-injected from zero to the rated voltage for all currents within the device rating. Wiik et al. developed in [87] a control method suitable for the LVRT application in transmission systems shown in Fig. 12 for injecting series voltage based on MERS equivalent compensating reactance expressed as

$$X_M = \frac{1}{\omega C}\left(1 - \frac{2\gamma}{\pi} - \frac{\sin 2\gamma}{\pi}\right) + \frac{4V_{C,\min}\cos\gamma}{\sqrt{2}\pi I_{grid}} \quad (4)$$

where I_{grid} is the line current and C in the capacitance of the dc capacitor.

3.1.5. Fault current limiter (FCL)

The need for FCL is increased by the rising fault current levels due to integration of high penetration of WTs into the power grids. In recent years, various types of FCL such as, solid state FCL, resonant circuit, transformer coupled bridge-type fault current limiter (BFCL), and superconducting fault current limiter (SFCL) have been proposed and developed [90–92].

Previous studies have proven the ability of SFCL and BFCL technology to improve LVRT capability and enhance transient stability of wind generator systems. By using these types of FCL during the fault, the stator current of induction generator has been effectively limited and the voltage reduction level of the generator terminals has been decreased, leading to meet international grid codes. Once, the FCL is adopted in the wind farm system, the peak value of short circuit current can be limited to a level within the switchgear rating, allowing deploying of light circuit breakers.

3.1.5.1. Bridge-type fault current limiter (BFCL). As shown in Fig. 14(a) and presented in [93,94], the bridge-type FCL with discharging resistor (R_{dc}) requires the coupling transformer to be connected to the power grid. A resistor in parallel with a semiconductor switch has been connected in series with the dc reactor (L_{dc}) of the conventional bridge-type FCL, in order to control the fault current level by controlling the dc reactor current. The increase of the fault current is curbed by dc reactor without any delay. This characteristic of the bridge-type FCL suppresses the instantaneous voltage drop and it is able to improve the transient behavior of WTs in fault instant, which is the main advantage of the bridge-type FCL to other FRT enhancement techniques [95]. Moreover, R_{dc} in the bridge-type FCL used to increase the terminal voltage of the generator, thereby smoothing the electrical torque and active output power fluctuations during the fault. However, this topology needs a special and costly transformer to connect the three-phase diode bridge in series into the system, in which primary voltage rating of the transformer must be almost equal to the transmission line voltage to maintain desired level of voltage within the fault duration [96].

In [96], the authors proposed a new modified configuration of BFCL including the four-diode bridge part and shunt resistive path, shown in Fig. 14(b), in order to achieve the LVRT of fixed speed wind generator system. In normal condition, the switch must be kept closed as its gate signal S_1 is at a high level, in which line current through the dc reactor placed within the diode bridge flows in the same direction, charging the L_{dc} to the peak current. Once the fault occurs, the sudden rise of fault current would be instantaneously limited by the reactor. Hence, abrupt voltage reduction at generator terminal is prevented during the fault, providing the improved transient behavior. Once, line current in dc side i_{dc} exceeds a predefined threshold i_{th}, the IGBT switch must be turned off via sending the low level signal to S_1. In this case, the diode bridge is cut off and the line current passes through the shunt resistor R_{sh} in order to suppress fault current and consumes excess energy from the wind generator. By controlling the duration of ON and OFF periods of IGBT switch, control system provides a manageable resistor in order to control the terminal voltage of

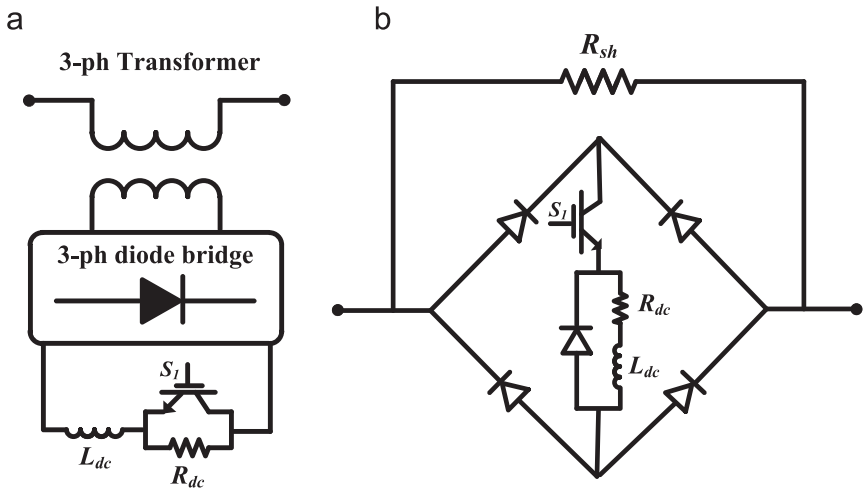

Fig. 14. Fault current limiter topology. (a) Bridge-type FCL (BFCL). (b) Modified configuration of BFCL.

induction generator, leading to a reduction in the rotor acceleration and stabilizing the system. The controller used for the BFCL was developed in [96] and shown in Fig. 15.

3.1.5.2. Superconducting fault current limiter (SFCL). The SFCLs have been launched and introduced into the network to restrict prospective fault currents immediately to a manageable level by suddenly raising the resistance value [97,98]. SFCL is considered as self-healing technology since it eliminates the need for any control action or human intervention due to its automatic excessive current detecting and automatic recovering from non-superconducting to superconducting states. By using the SFCL, the fault current is suppressed effectively and the voltage dip level of the WPP terminals is diminished, leading to enlarge the voltage safety margin of the LVRT curve [99–101]. The first-cycle suppression of a fault current by an SFCL results in an increased transient stability of the power system carrying higher power with greater stability. This innovating device introduces an exclusive feature that cannot be obtained by conventional current limitations.

Generally speaking, high temperature superconducting fault current limiters (SFCLs) have been classified into the resistive, inductive, and hybrid types [98]. Amongst diverse SFCL devices, resistive SFCL has a simple structure with a lengthy superconductor wire inserted in series with the transmission lines. To preserve the superconductor from detrimental hot spots during the operation, the shunt resistance, R_{shunt} is essential. This parallel resistance must be contacted all over the length of the superconductor, and it regulates the controlled current to elude overvoltages likely occurring when the resistance of the superconductor increases much quicker. With the recent breakthrough of economical second-generation high-temperature (HTS) wires, the SFCL has become more viable and is eventually expected to be at least a factor of ten lower in cost than presently available HTS conductor [102]. The structure of FSIG-based WT with resistive SFCL is schematically shown in Fig. 16. The current limiting behavior of the RSFCL can be modeled by the resistance transition of HTS tapes in terms of temperature and current density as defined by the following equation [100]:

$$R_{SFCL} = \begin{cases} 0 & \text{if} \quad J < J_c,\ T < T_c \quad \text{Superconducting state} \\ f\left(\left[\frac{J}{J_c}\right]^n\right) & \text{if} \quad J > I_c,\ T < T_c \quad \text{Flux flow state} \\ f(T) & \text{if} \quad T > T_c \quad \text{Normal state} \end{cases} \tag{5}$$

where J and T are the current density and temperature, respectively, while J_c and T_c are their critical values and n represents the exponent of $E-J$ power law relation.

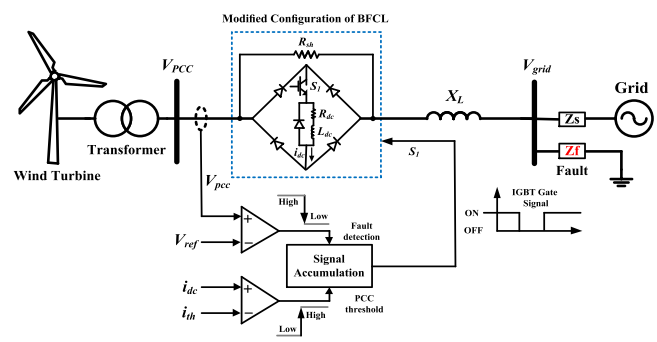

Fig. 15. Modified configuration of BFCL installed outside the wind farm with the control scheme.

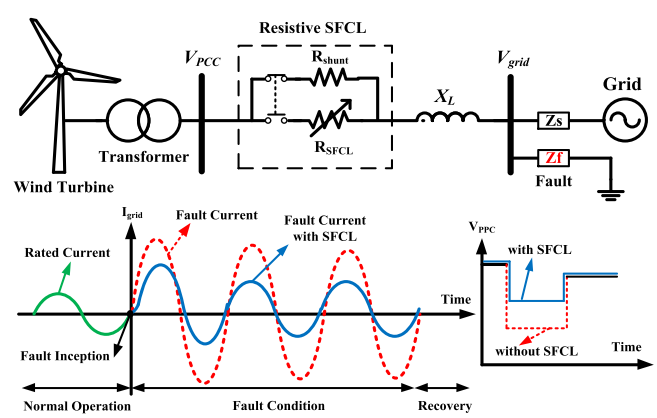

Fig. 16. Operation of resistive SFCL installed in transmission line including fault current and voltage profile at the wind turbine terminal.

3.2. Review on shunt-connected solutions

Among the external topologies, the shunt-connected devices have been widely utilized to provide smooth and fast steady state and transient voltage control at point of connection. Since, the output current of these devices is adjusted to control either the nodal voltage magnitude or reactive power injected at the voltage terminal, the shunt-connected topology proved to be the most effective solution in the wind power application in order to fulfill the recent international grid codes. A brief explanation of shunt-connected solutions is presented in following subsections.

3.2.1. Static var compensator (SVC)

Thyristor-controlled SVCs reported in [103,104], have been applied for voltage support of critical loads, reactive power compensation, and transient stability improvement in electric power transmission systems. The SVC is a combination of a thyristor-controlled reactor (TCR) with a thyristor-switched capacitor (TSC) or MSC as one compensator system which is practically connected to the PCC bus (or the wind turbine terminals) in order to provide fast voltage support and fulfill LVRT of WTs with induction generators [105–109].

Based on new grid codes, this is a supplementary feature now for wind turbines to supply variable reactive power depending on network demand and actual voltage level, while the crucial problem of SVC is to inject an uncontrollable reactive current dependently on the grid voltage [109]. Thus, the current injected by the SVC reduces linearly with the voltage sag and consequently the injected reactive power diminishes quadratically.

The basic control of the SVC was applied in [109] and shown in Fig. 17 as a PI controller to control the firing angle of the thyristors of the TCR and TSC, keeping V_{PCC} at 1 pu during and immediately after the fault. One key issue for designing of an SVC for proper operation is to tune the PI controller, which does not achieve in a simplistic method.

As discussed in [110], a fast response from the closed loop voltage control of the SVC can cause severe voltage oscillations under week grid operating, in which reduction of transient gain was proposed as a possible solution in order to diminish the SVC's response. However, tuning down the transient gain of SVC leads to a slower voltage recovery after the fault, thereby exceeding the LVRT requirements [111]. In [110], the authors implicitly promoted the idea of using several small distributed SVCs compared to a large central SVC for better voltage response with stable voltage oscillations. A Fuzzy controller was designed in [105] for the SVC to significantly prove an improved dynamic response in terms of overshoot and settling time as compared to a conventional PI controller.

3.2.2. Static synchronous compensator (STATCOM)

Unlike SVC, the STATCOM, also named SVC Light by ABB [37], can continuously and independently provides a controllable reactive current in response to voltage reduction, supporting the stability of grid voltage. The prospect of the STATCOM application in the wind power system has emerged in the 1990s, where its significant contribution was power quality improvement during normal operation [112]. The most important component of STATCOM is the modular voltage source converter (VSC), equipped with insulated gate bipolar transistors (IGBTs) that are controlled by pulse width modulation (PWM). Fig. 18 displays the basic STATCOM which can be used in LVRT capability for fixed-speed wind turbines.

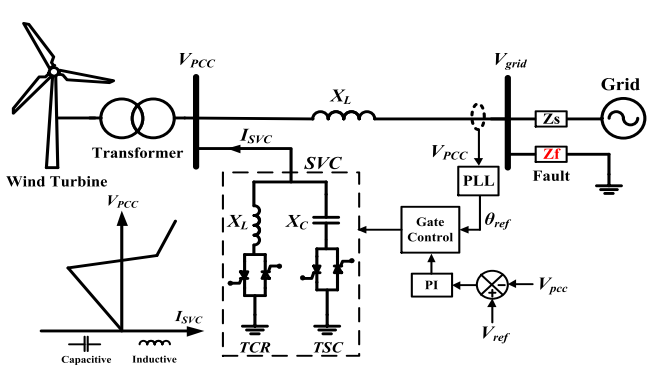

Fig. 17. Shunt compensation system for wind driven induction generator using SVC along with the basic control system.

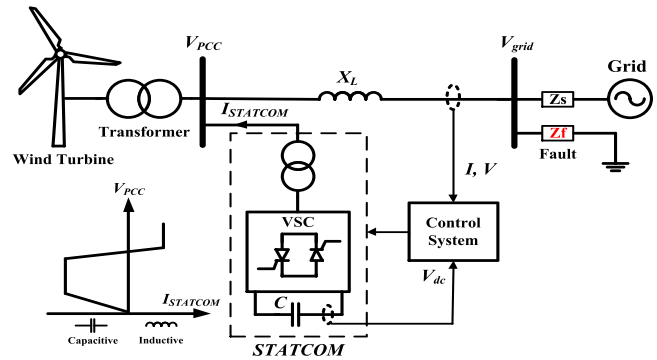

Fig. 18. The structure of the FSIG-based WT along with STATCOM connected to wind turbine terminal.

It is connected to the grid to inject or absorb reactive power through a three-phase transformer. This system is appropriate to alleviate the effects of both steady-state and transient contingencies [37]. Various papers have been documented in the literature [109,113–119] to prove the ability of STATCOM for LVRT enhancement of FSIG-based WT. In [109], Molinas et al. conducted a comparison between the STATCOM and SVC in terms of LVRT improvement. They found that STATCOM could be the economical solution in more situations (15% cheaper than SVC) if the same rating is assumed for the devices. A modified STATCOM controller was proposed in [115] based on the series combination of a power factor and a voltage regulation loop, which allows an optimized behavior of the fixed-speed WT both in normal and fault conditions. The feasibility of incorporating SDBR with STATCOM to fulfill LVRT requirement of FSWT was investigated in [120], where results showed that the less STATCOM rating was required compared to utilizing only STATCOM for the same effective performance. Since STATCOM is able to provide only reactive power, application of the energy storage system (ESS) with STATCOM have emerged as a promising solution for wind power system applications [116,121]. The new robust decentralized control system for large interconnected wind power system was introduced in [122] based on the linear quadratic (LQ) output-feedback control method to demonstrate that STATCOM/ESS structure can be an effective device for the grid-code compliant. Another alternative suggested in [123] was to simultaneously control both the reactive power and active power via the STATCOM and the pitch angle of the WT to ameliorate the LVRT capability of induction generators in wind farms. It was proved that the combined strategy of robust STATCOM and pitch angle control makes the system ride-through the fault without having to disconnect the generators from the system. However, utilizing the STACTOM for enhancing the LVRT capability augment the torque capability of the induction machine during the recovery process after the fault, causing in higher maximum torque, and correspondingly higher stresses on the drive-train. Therefore, authors in [117] suggested a solution based on indirect torque control (ITC) to temporarily set the voltage for the STATCOM controller to limit the maximum torque during the recovery.

3.2.3. Superconducting dynamic synchronous condenser (SDSC)

One possible solution of integrating large-scale wind farm in power system comprehensively presented in [124–127], is the superconducting dynamic synchronous condenser (SDSC) shown in Fig. 19(a), so that rotor windings entailed of HTS wires.

Compared with a conventional synchronous condenser, SDSCs provide up to 45% more dynamic reactive compensation in order to boost the bus voltage during a severe fault situation with power losses and maintenance (Fig. 19(b)). Since, SDSC machine has a relatively low synchronous reactance relatively low compared to

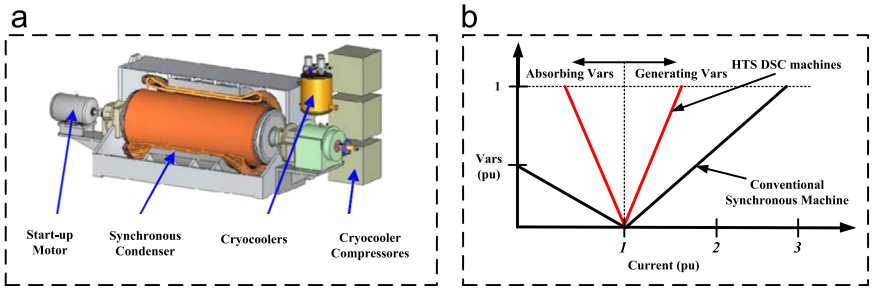

Fig. 19. The HTS DSC concept. (a) Structure of the SDCS. (a) Var curve for conventional synchronous and HTS DSC machines [126].

other synchronous machines with the same rating, allowing the machine to respond significantly to transient changes in voltage by injecting or absorbing reactive power. The SDSCs are able to perform with a very high field current (up to 2.0 pu) for a long period of time, allowing the machine to release the reactive power up to three-times rated output during a transient low-voltage event. Thus, the SDSC can assist a wind farm to meet the interconnection agreement with the utility by providing voltage regulation and improving stability of a power system [126].

3.3. Review on hybrid-connected solutions

Reactive power and voltage compensation using series–shunt (hybrid) topologies has been one of the effective techniques in improving the LVRT capability of the large scale of the wind farm level at the point of common coupling. The unified power quality conditioner (UPQC) demonstrates there may be a possible solution to the technical grid integration problems coming from the wind-driven FSIG [128–130]. Fundamentally, UPQC which is an integration of series and shunt VSC have been commonly studied by many researchers as the ultimate device to improve voltage sag, voltage unbalance, harmonics, dynamic active and reactive power regulation [131]. In [128], Jayanti et al. described the application of the UPQC systems to enhance low voltage ride-through capability of the FSIG-based wind turbine. The results show that series VSC provides the lack of voltage to prevent over-speeding of the FSIG while the shunt VSC injects additional VAR required during the voltage reduction.

However, the capital cost involved in the installation of this device is higher than any other solutions devices because of its use of two converters. Therefore, authors in [129] propose a novel combination of resistive SFCL and UPQC illustrated in Fig. 20, in order to improve power quality problems and fulfill grid code requirements. The obtained results confirm that the SFCL can not only reduce the volt-ampere rating of the UPQC, thereby reducing the installation cost, but also aid the LVRT capability of the wind turbine and improves dynamic performance of the induction generator for additional support.

Moreover, the feasibility of resistive SFCL incorporated in series with the dc-link inductance of the UPQC based on a current–source converter is proposed in [130] to limit excessive current in the event of the generator side fault (see Fig. 21) and increase voltage level at the generator terminal leading to compliance with international grid codes.

Huang et al. introduce in [132] a novel topology based on combined shunt and series grid interface configuration, namely, unified compensation system (UCS) to improve FRT capability for FSIG wind turbines. The system structure depicted in Fig. 22 utilizes one converter to provide both series and shunt compensation. In normal operation, the UCS operates like a STATCOM and supports voltage or reactive power regulation through the shunt connection. In faulty conditions, the UCS instantaneously switches

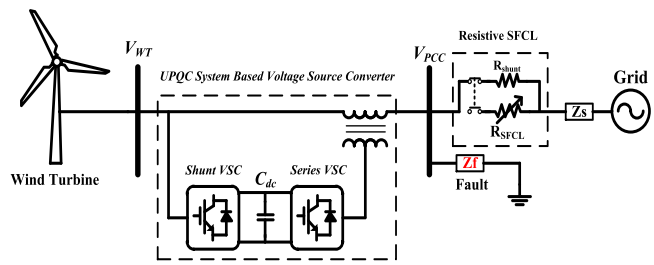

Fig. 20. The structure of the proposed system: FSIG-based wind turbine with UPQC and SFCL connected to the grid.

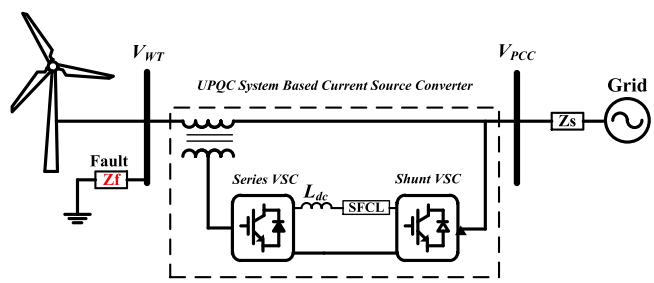

Fig. 21. The structure of the proposed system: FSIG-based wind turbine with current source UPQC and SFCL connected to the dc link.

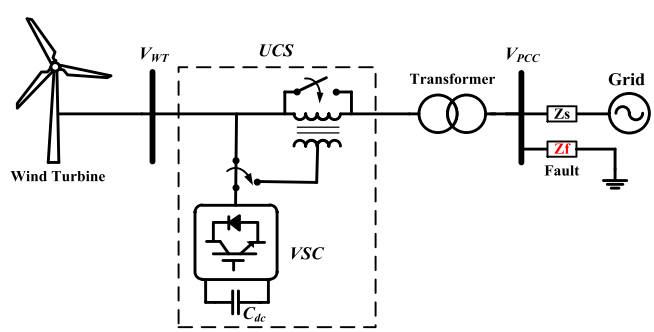

Fig. 22. Configuration of unified compensation system (UCS) connected to wind turbine terminal.

from the shunt to the series grid connection, compensates the voltage, and maintains the stator voltage at its rated value.

4. Technical–economical evaluation study of the LVRT methods

With regard to the above-described LVRT enhancement methods for the FSIG-based WT, no comparative studies have been considered between the different configuration schemes. In this

section, a comparative study of these LVRT methods in terms of dynamic performance and economic feasibility is performed.

4.1. Technical comparative study

Table 1 summarizes the advantages and limitations of applying the three categories of the LVRT schemes discussed in Sections 3.1–3.3. While the final aim of this summary is not to prioritize the LVRT enhancement methods based on technical features, it provides simple and clear metrics which could be used for decision making purposes.

The contributions of SVC and TCSC to transient voltage stability of the FSIG-based WT and power grid are presented in [65]. The comparative study verified that, in the case of wind speed fluctuation randomly, SVC can offer better reactive power compensation to maintain the transient stability, while TCSC can effectively promote the terminal voltage and enhance LVRT capability in the case of severe three-phase fault currents. Although TCSC and SVC have some sophisticated components such as thyristor, inductors and capacitors, they have relatively simple control structure. Compared with SVC, STATCOM provides faster response, fewer disturbances, and better performance at reduced voltage levels; as a result, it is the most extensively proposed solution for the ride-through capability enhancement of wind turbines based on FSIG. STATCOM may be rated for 75% of SVC rating for same performance in response to line fault [109]. STATCOM have a slightly smaller footprint than SVC because they use power electronics instead of capacitors and reactors. In [127], the authors studied a comparison between the SVC and SDSC in terms of voltage regulation in wind power applications. The results showed that the SVC has better dynamic performance during the fault with minor voltage reduction on the wind turbine terminal, while SDSC could adjust the voltage to the rated value faster during the severe faults such as three phase to ground faults. Among FATCS devices, although UPQC and UCS can exhibit superior performance due to the fact that they provide both series and shunt compensation, the overall cost and control complexity of these types of technologies are higher than other FACTS devices because of using two converters. However, compared with UPQC, UCS has less control complexity because only one converter is connected to the grid at the same time. The SDBR can be considered a very simple and cost-effective solution for LVRT capability enhancement of the wind generator system since it uses a high power resistor and fewer switches than other auxiliary methods. In [81], the direct comparison of SDBR and RPC for the fixed-speed WT was conducted, and demonstrated that a 0.05 pu dynamic resistor is equivalent to 0.4 pu of dynamic RPC. However, the SDBR can dissipate active power, but it cannot control reactive power; hence, it is unable to minimize voltage and power fluctuations of wind generator. Amongst diverse FCL devices, BFCL and SFCL technologies with simpler control structures have proven their ability to enhance LVRT capability and transient stability of WTs. However, BFCL needs a special and costly

Table 1
Technical comparison of LVRT improvement methods for FSIG-based WTs.

Methods		Main advantages	Main limitations	Notes(s)
Series connection	**TCSC** [60–67]	• Variable capacitive reactance • Useful for voltage unbalance and fault current limitation	• Undesirable resonance • Harmonic injection	• An effective solution for offshore wind farm
	DVR [68–79]	• Fast voltage recovery • Controllable reactive power supply	• Phase angle jump • Active power absorption	• Compatible with a proper energy storage capacity
	SDBR [80–85]	• Mechanical active power mitigation • Reduction of pitch angle activation • High reliability and low maintenance	• Unable to control reactive power • Unable to damp voltage fluctuations • Useless in low power factor usage	• 0.05 pu SDBR is equivalent to 0.4 pu of dynamic RPC for LVRT enhancement
	MERS [86–89]	• Eliminating reverse blocking switch • Effectiveness for large-scale application • Low switching losses	• Less robust control • Mechanical by-pass switch	• Capacitor is so smaller than a single-phase full bridge • Operating range is 71% larger than TCSC
	BFCL [93–96]	• Useful for high voltage drops • Minimizing rotor speed variations • Low conduction loss • No need to measure any parameters	• Needs a large-scale coupling transformer • Big reactance in huge application • Undesirable saturation of dc reactance	• Consumes more active power than the SDBR • Better performance than the SDBR in a sudden drop
	SFCL [97–102]	• Automatic fault current detecting • Automatic recovering • Fast fault current limiting action	• Unable to work at room temperature • Unable to control reactive power • High recovery time	• More feasible with second-generation of HTS wires.
Shunt connection	**SVC** [103–111]	• Reactive current injection • Voltage stability in weak system • Continuous voltage control	• Voltage-dependent reactive control • Unstable voltage oscillations due to faster response	• Inject more reactive power compared with SDSC with same capacity
	STATCOM [112,123]	• Controllable reactive current • Rapid response to disturbances • Negative-sequence voltage reduction	• Needs to cut off in a high voltage drop • Unable to supply active power	• Provide faster response and less disturbances compared with SVC
	SDSC [124–127]	• Able to perform with a very high current (up to 2.0 pu) for a long time • Low level of losses	• Less effective for low voltage drop	• Adjust the voltage faster than SVC • Provide 45% more reactive power compared to older types
Hybrid Connection	**UPQC** [128,131]	• Both active and reactive control • Fast reactive power compensation • Long critical clearance time	• Active power absorption • Needs a huge dc-link capacitor	• Share voltage control and reactive power control into the two VSC of the UPQC
	UPQC & SFCL [129,130]	• Fault current limiting action • Increasing the voltage safety margin of LVRT curve	• Difficulty in coordinating control scheme between SFCL and UPQC	• SFCL reduces the rating and cost of UPQC
	UCS [132]	• Supporting both shunt and series compensation with one converter	• High conduction losses of series bypass switch	• Behave like STATCOM in normal operation • Switch to the series grid interface in faulty condition

transformer to connect the three-phase diode bridge in series into the system.

4.2. Economical comparative study

This section further provides the economic study of all LVRT solutions to evaluate the complexities and economic feasibility of different existing LVRT methods. Economic considerations take into account the cost of wind power integration and the cost of allocated auxiliary devices for a range of operating conditions in terms of the cost per kW or kVar of implementation.

4.2.1. Wind power generation cost

The installed cost of a commercial wind power project is dominated by the capital cost for the wind turbines including blades, towers and transformer and this can be in the range of 65–84% of the total installed cost [133]. The other installed costs of a wind technology can be categorized into three groups, i.e., grid connection costs including transformers and substations (9–14%), civil works and construction costs (4–16%), and other capital cost including construction of buildings, control systems, project consultancy with costs share 4–10% of the total installed cost. The total installed capital costs for wind technology vary significantly depending on the energy market and the local cost structure. China and India have the lowest installed capital costs for new onshore projects of between USD 1100/kW and USD 1400/kW in 2010 and in the range USD 1850 to USD 2200 in the major developed country markets of the United States, Germany and Spain. Fig. 23 presents the assumptions for onshore wind capital costs for typical projects in Europe, North America and China/India for 2010 and 2011, as well as the predicted values for 2015 [133]. Moreover, additional LVRT technologies impact the operation of WT technology economically and technically. Although the actual costs of the auxiliary devices are not widely available, using existing reported data from commissioned projects, the overall cost of these technologies can be roughly estimated. The overall cost of LVRT solutions can be obtained based on their major components such as number of power electronic switches used, coupling transformer, magnetic inductance, high power resistance, capacitor etc.

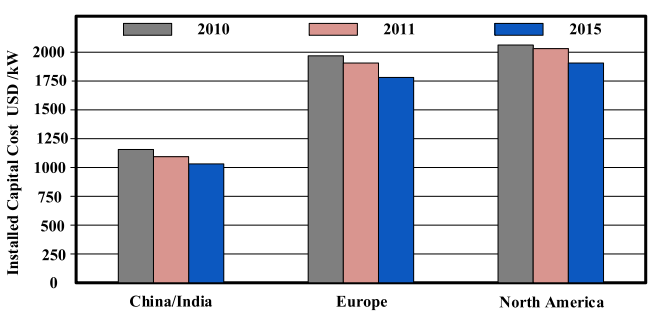

Fig. 23. Installed cost of wind power projects in three area; 2010, 2011, and 2015.

4.2.2. Economic feasibility of LVRT solutions

The growing integration of wind generation in power grids, is expected to surge the demand of FACTS in different geographies. The overall FACTS market is projected to reach $1386.01 million by 2018 from the $912.85 million that it accounted for in 2012 [134]. SVC is the most widely used solution in the global market, followed by the Fixed Series Capacitors (FSC); whereas devices such as STATCOM and UPFC are customized solutions made for special requirements of the power grids. Obviously, FACTS-based methods are the relatively expensive because they consist of many components such as power electronic devices, thyristors, reactors, capacitor banks, switchgear, protection and control systems, and so on. In this section, the cost range of the major FACTS devices is mostly taken from the Siemens and electric power research institute (EPRI) database reported in [135–137], as shown in Fig. 24(a, b).

Accordingly, the cost functions for TCSC, SVC, STATCOM and UPFC are developed as follows:

$$\begin{cases} \cos t_{TCSC} = 0.0015s^2 - 0.713s + 153.75 & \text{US\$/kVar} \\ \cos t_{SVC} = 0.003s^2 - 0.305s + 127.38 & \text{US\$/kVar} \\ \cos t_{STACOM} = 0.003s^2 - 0.233s + 153.45 & \text{US\$/kVar} \\ \cos t_{TCSC} = 0.003s^2 - 0.269s + 188.22 & \text{US\$/kVar} \end{cases} \tag{6}$$

where s is the operating range of FACTS devices in MVar. The marginal cost per installed kVar of the FACTS devices decreases as the operating rate capability is increased. An overall cost for a 100-MVar SVC and a 100-MVar TCSC varies from USD 60 to USD 100 per kVar and USD 70 to USD 95 per kVar, respectively. Although TCSC and SVC have some sophisticated components such as thyristor, inductors and capacitors, they have relatively simple control structure. Similarly, based on Fig. 23, the overall cost for STATCOM and UPFC varies from USD 100 to USD 130 per kVar and USD 130 to USD 170 per kVar at 100 MVar rating of the operation, respectively. A cost analysis has been reported for the DVR in [138–139], where the overall cost including series transformers, VSC using IGBT, and capacitor bank is estimated between around $130/kVar and $150/kVA at operating rate of 100 MVar. This research service provides revenue forecasts for the total dynamic voltage restorer (DVR) markets as well as for low voltage and medium voltage restorers. The demand for DVR equipment is set the global DVR markets to grow at 6.9% between 2004 and 2011,

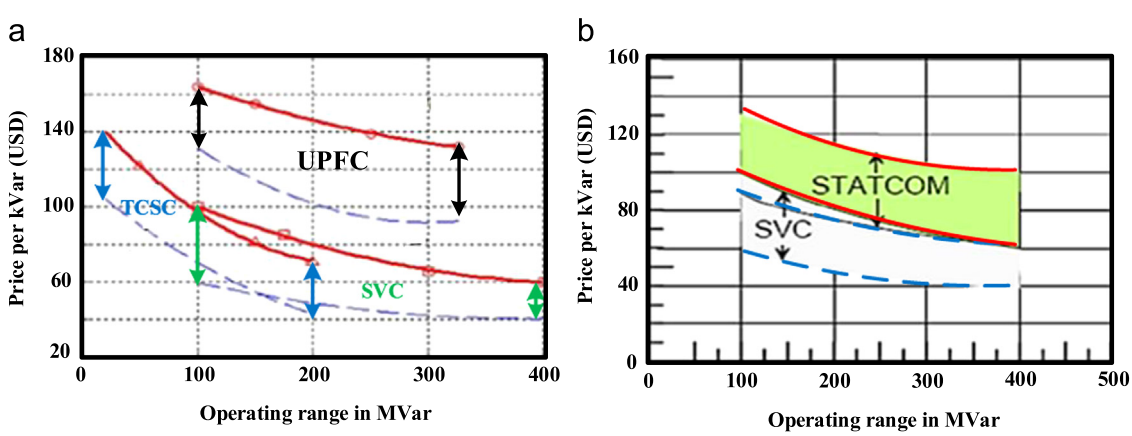

Fig. 24. An operating cost comparison between FACTS devices. (a) SVC, TCSC, and UPFC [135]. (b) SVC and STATCOM [137].

the growth being more prominent in North America and Asia Pacific. Spanish company CONVERTDIP has successfully put their related products into markets, which is called W2PS [140].

The 8-MVar SDSC machine, developed by American Superconductor, was demonstrated at the Tennessee Valley Authority (TVA) in Gallatin in order to dynamically absorb or produce reactive power, costing between $1 million and $1.2 million [141].

Due to its compact size and low-cost design, the total cost of the SDSC can be reached up to USD 100/kVar for operating range of 100 MVar or more. Because of high efficiency and the low maintenance cost of the new HTS dynamic synchronous condenser it is a very economic option for providing peak and dynamic reactive compensation to a power system. Also, at the present time, the cost of superconducting materials and the cryogenic cooling system of the SFCL are extremely high (up to $200,000@800 W/2.5 kA [142]); thus, to maintain economic feasibility of the final product, the market trend is to minimize the amount of HTS material needed. With the recent breakthrough of economical second-generation HTS wires, the SFCL has become more viable and is eventually expected to be at least ten USD less in cost than presently available HTS conductors [143]. The average energy dissipated by SDBR determines its size and cost, so that power rating of the SDBR chosen to be greater than average energy dissipated. Once these values are determined, the resistors can be chosen. ABB represented a multi-level structure, call their products Transient Booster® [85]. Multistage resistors increase the cost and complexity of SDBR, while single-stage mechanical switching as the lowest cost and least complex option with high reliability and low maintenance and, as a result, single stage SDBR in comparison with FACTS devices may be a preferred solution.

Although study of the SDBR, MERC and the BFCL cost are unreported, but based on the complexity of the controller and the configuration of them, SDBR can be easily considered as cheapest solution for LVRT improvement after the capacitor bank. The cost of MERC and BFCL can also be estimated as LVRT solutions that are less costly than FACTS devices because they do not require series transformer, sophisticated power electronic converters, or energy storage. As stated in Section 3.1.4, the dc-link capacitor of the MERS is several times smaller than that of a regular single-phase full bridge inverter. Thus, between MERS and STATCOM with the same topology, the MERC might be cheaper. Since the economical scope of this section is to only compare the average and estimated overall costs of all LVRT solutions for FSIG-based WT, the range of prices (US$) per kVar is shown in Fig. 25.

5. Simulation results and performances comparison

As stated in Section 3 and shown in Table 1, the presented LVRT capability enhancement methods for FSIG-based WTs hold some advantages and limitations. To verify effectiveness of the described methods and also to compare them, some simulation studies using MATLAB/SIMULINK software were carried out in this section. The single-line diagram of the proposed power system, including a large wind farm, a hydro power represented by a synchronous generator, and possible shunt and series connected compensators is schematically shown in Fig. 26. As arbitrary choices, the most common series and shunt connected RPC devices, i.e., STATCOM, SVC, TCSC, and DVR, are applied at the terminal of the wind generator. The parameters of the grid components, FSIG, and RPC devices are given in Tables 2–4 in Appendix. For comparison purposes, the dynamic performance of the combinatorial wind farm and auxiliary devices were compared with the cases without the compensation scheme. A three-phase symmetrical grid fault is considered, since the fault ride-through capability of the regional grid codes mostly refer to this type of fault. Thus, a three-phase

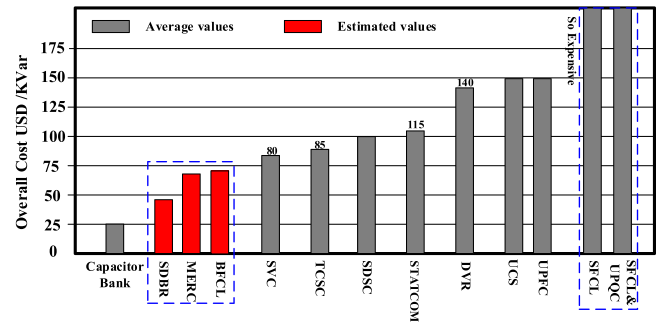

Fig. 25. Average and estimated overall cost of LVRT solutions for operating range of around 100 MVar.

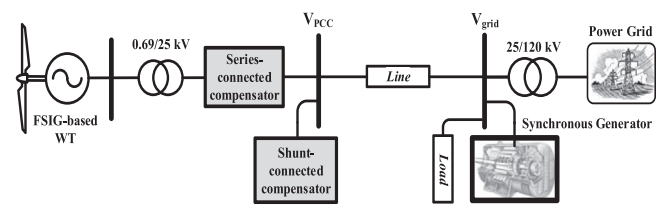

Fig. 26. Single-line diagram of the power network including a series-connected or shunt-connected compensator.

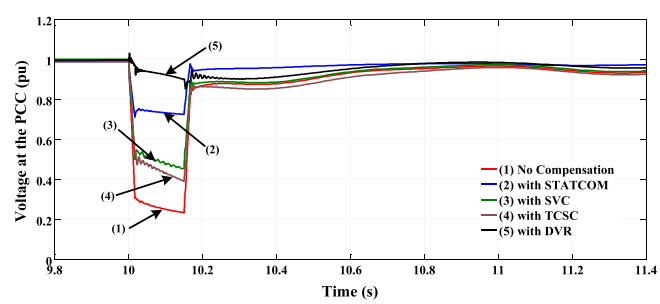

Fig. 27. FSIG terminal voltage at PCC.

fault is applied at $t=10$ s and is cleared after 150 ms, resulting in 80% voltage dip at the PCC. The responses of the terminal voltage (PCC), active and reactive power, stator current, and rotor speed of the FSIG are shown in Figs. 27–31, respectively. Although all auxiliary devices can meet the LVRT capability requirements of the wind generator, their performance varies with their behavior and capabilities.

It is clear that among the described methods, the performances of the STATCOM and DVR are the best and can effectively stabilize the wind generator system, while TCSC exhibits the worst performance; yet it can enhance the LVRT compared with the "No Compensation" case.

Fig. 27 shows voltage at the PCC in different methodologies. Among the described methods, DVR method has superior performance for diminishing the voltage dip during the fault, where voltage can be significantly retained to around 1 pu, using STATCOM after clearing the fault. Since quick voltage recovery is very important for an FSIG-based WT wind turbine, STATCOM is a very useful method to provide the quick reactive power and voltage control.

The performance of TCSC and SVC methods are approximately similar and these methods allow wind turbines to handle only a fraction of the total FSIG active power. Fig. 28 depicts wind turbine active power during and after clearing the voltage sag. During the fault, the machine output active power becomes almost zero with no compensation. But STATCOM helps maintain more than half of

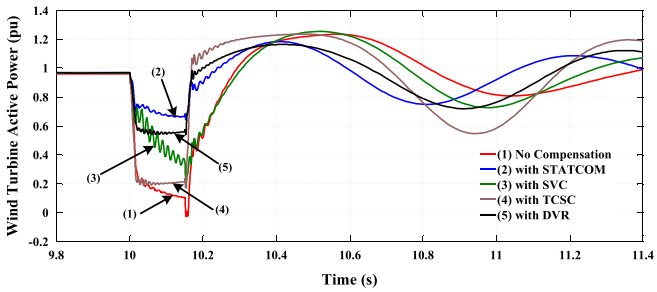

Fig. 28. FSIG active power output at PCC.

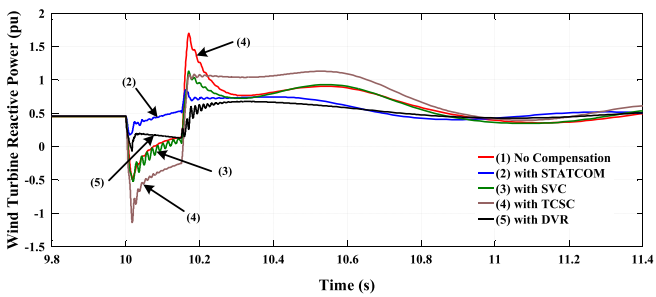

Fig. 29. Reactive power absorbed by FSIG.

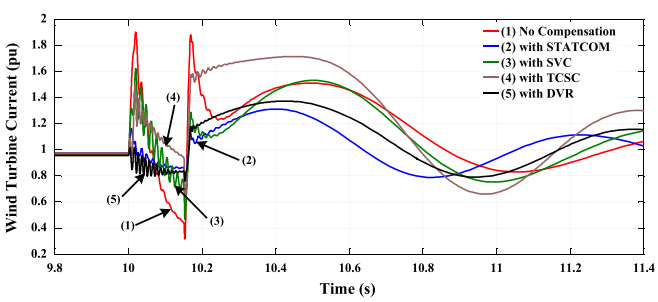

Fig. 30. Stator current of the FSIG.

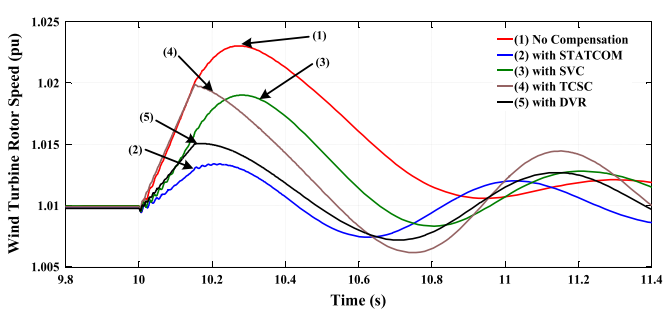

Fig. 31. FSIG rotor speed.

the rated active power at the PCC during the fault. Although the DVR method has the best performance in PCC voltage regulation, when the DVR compensates for the voltage sag; some portion of the wind turbine active power is partly fed into the DVR system, resulting in less active power transferred to the grid.

Fig. 29 illustrates total reactive power absorbed by the FSIG from the network. After fault clearing (at $t=10.15$ s), the generator needs to draw a large amount of reactive power to re-establish the magnetic field, which leads to a lower voltage at the terminal of the WT system. However, compared with the no compensation case, the absorbed reactive power from the grid is significantly reduced with the STATCOM and DVR, which helps to avoid other problems such as voltage collapse and recovery process.

Machine speed response and stator current of the FSIG are shown in Figs. 30 and 31, respectively. As it can be seen, the rotor speed and stator current increases during the fault period which may lead to power system instability and is detrimental for the turbine generator system if the fault duration is long and proper auxiliary devices are not used (no controller). Similarly, STATCOM and DVR can limit the rate of rising of machine speed and the magnitude of the machine current in order to make better stability.

6. Conclusions

This paper presented the comprehensive review of the state-of-the-art developments for LVRT capability improvement of WTs based on fixed-speed wind turbines, which is relatively a new concept in maintaining voltage profile of the wind power generation. First, the responses of the FSIG under steady-state and transient-state condition were extensively discussed. Then, all reviewed methodologies were categorized into three main groups, i.e., series-connected solutions, shunt-connected solutions, and hybrid-connected solutions; discussing the performance of the LVRT schemes including their advantages and limitations in details. Also, a comprehensive analysis of these LVRT methods in terms of dynamic performance, controller complexity, and economic feasibility was comparatively investigated and summarized in Table 1. It is found that the overall cost and control complexity of the SFCL and UPQC schemes are higher than other types of LVRT technologies. On the other hand, the SDBR and BFCL methods were relatively the cheapest and simplest control structure among other LVRT solutions from economic feasibility point of view. Finally, some selected case studies were simulated using the MATLAB/Simulink software. Comparison of simulated methods indicated that DVR from series-connected solutions and STATCOM from shunt connected solutions are the most reliable and effective LVRT capability enhancement methods, while TCSC exhibited the worst performance; yet it can enhance the LVRT compared with no LVRT controller employed with FSIG-based WT. Although the market share in the conventional fixed-speed wind turbine concept has diminished, nevertheless a non-negligible 20% of the existing wind energy in Europe is still employing FSIGs due to their simple structure and lower maintenance cost. Thus, this effort helps the researchers understand the relative effectiveness of the proposed auxiliary equipment and provides a guideline for selecting a suitable technique for the LVRT capability improvement of wind turbine generator systems.

Appendix A

See Tables 2–4

Table 2
FSIG-based WT parameters.

Wind turbine parameters	Values	FSIG parameters	Values
Rated turbine power	3 MW	Rated power	3 MW
Rated wind speed	10 m/s	Rated voltage	0.69 kV
Blade radius	44 m	Stator resistance	0.0048 pu
Optimal power coefficient	0.45	Rotor resistance	0.0044 pu
Optimal tip speed ratio	8.32	Stator inductance	0.125 pu
Rotor speed	1.2 pu	Rotor inductance	0.179 pu

Table 3
FSIG-based WT parameters.

Parameters of the grid	Values
Rated voltage	120 kV
Rated frequency	60 Hz
Transmission line	$0.11+j0.001$ pu
Load	2 MW
Rated SG power	5 MW
Rated SG voltage	25 kV

Table 4
Parameters of FACTS devices.

Parameters of STATCOM	Values	Parameters of TCSC	Values
Rated power	3 MVar	Rated power	3 MVar
Transformer voltage	2.5/25 kV	Rated voltage	25 kV
dc-Link voltage	2760 V	Capacitance	21.91 uF
dc-Link capacitance	0.02 F	Reactance	0.043 H
Parameters of SVC	**Values**	**Parameters of DVR**	**Values**
Rated power	3 MVar	Rated power	3 MVar
Transformer voltage	2.5/25 kV	Transformer voltage	2.5/25 kV
Rated capacitor power	3 MVar	dc-Link voltage	2700 V
Rated inductance power	1.5 MVar	dc-Link capacitor	6 mF

References

[1] Dilip A, Marika T. Sustainable energy for developing countries. S.A.P.I.EN.S. [Online]. 2009; 2(1):1–16.
[2] Liu TY, Tavner PJ, Feng Y, Qiu YN. Review of recent offshore wind power developments in china. Wind Energy 2013;16(5):786–803.
[3] Renewable energy technologies: cost analysis series. International renewable energy agency (IRENA); 2012.
[4] Mohammad SN, Das, NK, Roy S. A review of the state of the art of generators and power electronics for wind energy conversion systems. In: Proceedings of the 2014 3rd international conference on the developments in renewable energy technology (ICDRET); 2014. p. 29–31.
[5] Muyeen SM, Takahashi R, Murata T, Tamura J. A variable speed wind turbine control strategy to meet wind farm grid code requirements. IEEE Trans Power Syst 2010;25(1):331–40.
[6] Leon AE, Mauricio JM, Gomez A, Solsona JA. An improved control strategy for hybrid wind farms. IEEE Trans Sustain Energy 2010;1(3):131–41.
[7] Qiuwei Wu, Zhao Xu, Østergaard J. Grid integration issues for large scale wind power plants (WPPs). In: Proceedings of the power and energy society general meeting; 2010. p. 25–9.
[8] Syed MH, Zeineldin HH, El Moursi MS. Hybrid micro-grid operation characterization based on stability and adherence to grid codes. IET Gener Transm Distrib 2014;8(3):563–72.
[9] Grid code high and extra high voltage. Tech. Rep., E.ON NetzGmgH Bayreuth [Online]; 2003. Available: ⟨http://eon-netz.com/⟩.
[10] Eltra specifications, wind farms connected to the grid with voltages over 100 kV: technical regulations for the properties and control of wind turbines. Tech. Rep., Eltra Corp.; 2004.
[11] Rahmann C, Haubrich HJ, Moser A, Palma-Behnke R, Vargas L, Salles MB. Justified fault-ride-through requirements for wind turbines in power systems. IEEE Trans Power Syst 2011;26(3):1555–63.
[12] Barry D. Increasing renewable energy accessibility in Ireland. In: Proceedings of the 19th world energy congress; 2004. p. 1–10.
[13] Kyaw MM, Ramachandaramurthy VK. Fault ride through and voltage regulation for grid connected wind turbine. Renew Energy 2011;36(1):206–15.
[14] Federal Energy Regulatory Commission (FERC), United States of America, Docket No. RM05-4-000 – Order No. 661. Interconnection for Wind Energy. Issued June 2, 2005.
[15] Kamel RM. Three fault ride through controllers for wind systems running in isolated micro-grid and effects of fault type on their performance: a review and comparative study. Renew Sustain Energy Rev 2014;37:698–714.
[16] Grid connection of wind turbines to networks with voltages below 100 kV. Regulation TF 3.2.6, Energinet, Fredericia, Denmark; May 2004.
[17] Ellis A, Nelson R, Von Engeln E, Walling R, MacDowell J, Casey L, et al. Review of existing reactive power requirements for variable generation. In: Proceedings of the power and energy society general meeting; 2012. p. 22–6.
[18] FERC Standard Large Generator Interconnection Agreement (LGIA), [Online]; June 16, 2005. Available: ⟨www.ferc.gov/industries/electric/indus-act/gi/stnd-gen/2003-C-LGIA.doc/⟩.
[19] Mohseni M, Islam SM. Review of international grid codes for wind power integration: diversity, technology and a case for global standard. Renew Sustain Energy Rev 2012;16(6):3876–90.
[20] Dowds J, Hines P, Ryan T, Buchanan W, Kirby E, Apt J, Jaramillo P. A review of large-scale wind integration studies. Renew Sustain Energy Rev 2014;49:768–94.
[21] Etxegarai A, Eguia P, Torres E, Iturregi A, Valverde V. Review of grid connection requirements for generation assets in weak power grids. Renew Sustain Energy Rev 2015;41:1501–14.
[22] De Alegria IM, Andreu J, Martin JL, Iban P, Villate JL, Camblong H. Connection requirements for wind farms: a survey on technical requirements and regulation. Renew Sustain Energy Rev 2007;11(8):1858–72.
[23] Tsili M, Papathanassiou S. A review of grid code technical requirements for wind farms. IET Renew Power Gener 2009;3(3):308–32.
[24] Flannery P, Venkataramanan G. Unbalanced voltage sag ride-through of a doubly fed induction generator wind turbine with series grid side converter. IEEE Trans Ind Appl 2009;45(5):1879–87.
[25] Santos-Martin D, Rodriguez-Amenedo JL, Arnaltes S. Providing ride-through capability to a doubly fed induction generator under unbalanced voltage dips. IEEE Trans Power Electron 2009;24(7):1747–57.
[26] Yaramasu V, Bin Wu, Alepuz S, Kouro S. Predictive control for low-voltage ride-through enhancement of three-level-boost and NPC-converter-based PMSG wind turbine. IEEE Trans Ind Electron 2014;61(12):6832–43.
[27] Sasikumar M, Chenthur Pandian S. Performance characteristics of self-excited induction generator fed current source inverter for wind energy conversion applications. Int J Comput Electr Eng 2010:1793–8163.
[28] Holdsworth L, Wu XG, Ekanayake JB, Jenkins N. Comparison of fixed speed and doubly-fed induction wind turbines during power system disturbances. IET Proc Gener Transm Distrib 2003;150(3):343–52.
[29] Nasiri M, Milimonfared J, Fathi SH. A review of low-voltage ride-through enhancement methods for permanent magnet synchronous generator based wind turbines. Renew Sustain Energy Rev 2015;47:399–415.
[30] Justo JJ, Mwasilu, Jung JW. Doubly-fed induction generator based wind turbines: a comprehensive review of fault ride-through strategies. Renew Sustain Energy Rev 2015;15:447–67.
[31] Rahimi M, Parniani M. Grid-fault ride-through analysis and control of wind turbines with doubly fed induction generators. Electr Power Syst Res 2009;80(2):184–95.
[32] Hussein A, Hasan Ali M. Comparison among series compensators for fault ride through capability enhancement of wind generator systems. Int J Renew Energy Res 2014;4(3):124–34.
[33] Hansen LH, Helle L, Blaabjerg F, Ritchie E, MunkNielsen S, Bindner H, et al. Conceptual survey of generators and power electronics for wind turbines Tech. Rep. Riso-R1205 (EN). Roskilde, Denmark: Risø Nat. Lab.; 2001.
[34] Anaya-Lara O, Jenkins N, Ekanayake J, Cartwright P, Hughes M. Wind energy generation modeling and control. Wiley; 2009.
[35] Blaabjerg F, Chen Z, Kjaer SB. Power electronics as efficient interface in dispersed power generation systems. IEEE Trans Power Electron 2004;19(5):1184–94.
[36] Chen Z, Blaabjerg F. Wind turbines: a cost effective power source. Przeglad Elektrotechniczny 2004:464–9.
[37] Zhe C, Guerrero JM, Blaabjerg F. A review of the state of the art of power electronics for wind turbines. IEEE Trans Power Electron 2009;24(8):1859–75.
[38] Sathyajith Mathew. Wind energy: fundamentals, resource analysis and economics. Springer Science & Business Media; 2006.
[39] Akhmatov V, Knudsena H, Nielsen AH, Pedersenb JK, Poulsenc NK. Modeling and transient stability of large wind farms. Int J Electr Power Energy Syst 2003;25(2):123–44.
[40] Bianchi FD, Mantz RJ, Christiansen CF. Gain scheduling control of variable speed wind energy conversion systems using quasi-LPV models. Control Eng Pract 2005;13(2):247–55.
[41] Rocha R, Filho LSM. A multivariable control for wind energy conversion system. In: Proceedings of the IEEE conference on control applications; 2003. p. 206–11.
[42] Chedid R, Mrad F, Basma M. Intelligent control of a class of wind energy conversion systems. IEEE Trans Energy Convers 1999;14(4):1597–604.
[43] Ragheb AM, Ragheb M. In: Dr. Rupp Carriveau, editor. Wind turbine gearbox technologies, fundamental and advanced topics in wind power; 2011. Available: ⟨http://www.intechopen.com/books/fundamental-and-advanced-topics-in-wind-power/wind-turbine-gearboxtechnologies⟩.
[44] Sumper A, Bellmunt O, Anddreu A, Robles R, Duran J. Response of fixed speed wind turbines to system frequency disturbance. IEEE Trans Power Syst 2009;24:181–92.
[45] Bansal RC. Three-phase self-excited induction generators: an overview. IEEE Trans Energy Convers 2005;20(2):292–9.
[46] Dixon J, Moran L, Rodriguez J, Domke R. Reactive power compensation technologies: state-of-the-art review. Proc IEEE 2005;93(12):2144–64.
[47] Kanabar M, Khaparde S. In: Dr. Ibrahim Al-Bahadly, editor. Rotor speed stability Analysis of a constant speed wind turbine generator. Wind turbines. Available: ⟨http://www.intechopen.com/books/wind-turbines/rotor-speed-stability-analysis-of-a-constantspeed-wind-turbine-generator⟩.

[48] Tamura J, Analysis of transient stability of wind generators. In: Proceedings of the international conference on electrical machines (ICEM); 2002.
[49] Slootweg JG, Haan SWD, Polinder H, Kling WL. General model for representing variable speed wind turbines in power system dynamics simulations. IEEE Trans Power Syst 2003;18(1):144–51.
[50] Muyeen SM, Ali MH, Takahashi R, Murata T, Tamura J. Transient stability enhancement of wind generator by a new logical pitch controller. IEEE Trans Power Energy 2006;126(8):742–52.
[51] Muljadi E, Butterfield CP. Pitch-controlled variable-speed wind turbine generation. IEEE Trans Ind Appl 2001;37(1):240–6.
[52] Joseph Kearney. Grid voltage unbalance and the integration of DFIG. A thesis submitted for the degree of Doctor of Philosophy to the Dublin Institute of Technology; 2013.
[53] Piwko R, Miller N, Gasca, JS, Yuan X, Dai R, Lyons J. Integrating large wind farms into weak power grids with long transmission lines. In: Proceedings of the power electronics and motion control conference, vol. 2; 2006. p. 1–7.
[54] Gomis-Bellmunt O, Junyent-Ferre A, Sumper A, Bergas-Jan J. Ride-through control of a doubly fed induction generator under unbalanced voltage sags. IEEE Trans Energy Convers 2008;23(4):1036–45.
[55] Muljadi E, Yildirim D, Batan T, Butterfield CP. Understanding the unbalanced-voltage problem in wind turbine generation. Ind Appl Conf 1999;2:1359–65.
[56] Wessels C, Hoffmann N, Molinas M, Fuchs FW. StatCom control at wind farms with fixed-speed induction generators under asymmetrical grid faults. IEEE Trans Ind Electron 2013;60(7):2864–73.
[57] Wessels C, Hoffmann N, Molinas M. Voltage control of a STATCOM at a fixed speed wind farm under unbalanced grid faults. In: Proceedings of the 37th IEEE IECON; 2011. p. 979–84.
[58] Næss BI, Undeland TM, Gjengedal T. Methods for reduction of voltage unbalance in weak grids connected to wind plants. In: Wind power and the impact on power systems IEEE-Cigre workshop; 2002.
[59] Singh B, Murthy S, Gupta S. StatCom-based voltage regulator for self-excited induction generator feeding nonlinear loads. IEEE Trans Ind Electron 2006;53(5):1437–52.
[60] Kadia JV, Jamnani JG. Modeling and analysis of TCSC controller for enhancement of transmission network. Int J Emerg Technol Adv Eng 2012:2250–459.
[61] Del Rosso A, Cañizares CA, M., Doña V. A study of TCSC controller design for power system stability improvement. IEEE Power Energy Soc 2003.
[62] Mattavelli P, Verghese GC, Stankovi AM. Phasor dynamics of thyristor-controlled series capacitor systems. IEEE Trans Power Syst 1997;3(12):1259–67.
[63] Bachmann U, Berger F, Reinisch R, Erlich I, Häusler M, Lösing M, et al. Possibilities of multifunctional FACTS application in European electric power system under the changing conditions of the liberalized electricity market. CIGRE 2002.
[64] Paserba JJ. How FACTS controllers benefit AC transmission systems. In: Proceedings of the power engineering society general meeting; 2004. p. 1257–62.
[65] Zhou H, Wei H, Qiu X, Xu J, Wei X, Wang S. Improvement of transient voltage stability of the wind farm using SVC and TCSC. In: Proceedings of the power and energy engineering conference (APPEEC); 2011. p. 25–8.
[66] Joshi NN, Mohan N. Application of TCSC in wind farm application. In: Proceedings of the international symposium on power electronics, electrical drives, automation and motion; 2006. p. 23–6.
[67] Larsen EV, Clark K, Miske SA, Urbanek J, et al. Characteristics and rating considerations of thyristor controlled series compensation. IEEE Trans Power Deliver 1994;9:992–1000.
[68] Gaztanaga H, Etxeberria IO, Bacha S, Roye D. Fixed speed wind farm operation improvement by using DVR devices. In: Proceedings of the IEEE international symposium on industrial electronics; 2007. p. 2679–84.
[69] Visiers M, Mendoza J, Búnez J, González F, Contreras A, Molina S, et al. Windfact, a solution for the grid code compliance of the wind farms in operation. In: Proceedings of the European conference on electronics and applications; 2007:1–9.
[70] Ramirez D, Martinez S, Platero CA, Blazquez F, de Castro RM. Low-voltage ride-through capability for wind generators based on dynamic voltage restorers. IEEE Trans Energy Convers 2011;26(1):195–203.
[71] T, Kara A, Rahmani M, Westermann D. Power quality ensured by dynamic voltage correction. ABB Rev 1998;4:25–36.
[72] Sezi T. Kompensation von spannungseinbrüchen im mva-lastbereich. Etz 2001;9:20–3.
[73] Meyer C, Doncker RW, Li YW, Blaabjerg F. Optimized control strategy for a medium-voltage DVR—theoretical investigations and experimental results. IEEE Trans Power Electron 2008;23(6):2746–54.
[74] Bollen MH. Understanding power quality problems—voltage sags and interruptions. New York: IEEE Press; 2000.
[75] Sivasankar G, Kumar VS. Improving low voltage ride through capability of wind generators using dynamic voltage restorer. J Electr Eng 2014;65(4):235–41.
[76] Meyer C, De Doncker RW, Li YW, Blaabjerg F. Optimized control strategy for a medium-voltage DVR-theoretical investigations and experimental results. IEEE Trans Power Electron 2008;23(6):2746–54.
[77] Joshi N, Mohan N. A novel scheme to connect wind turbines to the power grid. IEEE Trans Energy Convers 2009;24(2):504–10.
[78] Chen WL, Wang MJ. Control design of a dynamic voltage restorer for wind-driven induction generators during a low voltage fault at grid bus. Electr Power Compon Syst 2014:1553–64.
[79] Li YW, Mahinda D, Blaabjerg F, Loh PC. A robust control scheme for medium-voltage-level DVR implementation. IEEE Trans Ind Electron 2007;54(4):2249–61.
[80] Causebrook A. Dynamic braking of electric generators for fault ride-through control. U.K. Patent Application no. GB0526133.4. Newcastle University; 2004.
[81] Causebrook A, Atkinson DJ, Jack AG. Fault ride-through of large wind farms using series dynamic braking resistors. IEEE Trans Power Syst 2007;22(3):966–75.
[82] Causebrook A, Atkinson DJ, Jack AG. Low voltage ride-through: shifting the balance of power from blade pitch to electrical resistance. In: Proceedings of the European wind energy conference; 2006.
[83] Freitas W, Morelato A, Xu W. Improvement of induction generator stability using braking resistors. IEEE Trans Power Syst 2004;19(2):1247–9.
[84] Causebrook A. Fault ride through of wind farms using series dynamic braking resistors [Ph.D. dissertation]. Department of EEC Engineering, NCL University; 2008.
[85] Gertmar L, Christensen HC, Nielsen EK, Wraae LE, et al. New method and hardware for grid connection of wind turbines and parks. In Proceedings of the Copenhagen offshore wind conference and exhibition, Copenhagen; 2005.
[86] Wiik JA, Widjaya FD, Isobe T, Kitahara T, Shimada R. Series connected power flow control using magnetic energy recovery switch (MERS). In Proceedings of the power conversion conference, Nagoya; 2007. p. 983–90.
[87] Wiik JA, Fonstelien OJ, Shimada R. A MERS type series FACTS controller for low voltage ride through of induction generators in wind farms. In Proceedings of the 13th European conference on power electronics and applications, Spain; 2009. p. 1–10.
[88] Wiik JA, Wijaya FD, Shimada R. An innovative series connected power flow controller. Magnetic Energy Recovery Switch (MERS). In: Proceedings of the power engineering society general meeting; 2007. p. 24–8.
[89] Wiik JA, Wijaya FD, Shimada R. Characteristics of the magnetic energy recovery switch (MERS) as a series FACTS controller. IEEE Trans Power Deliver 2009;24(2):828–36.
[90] Fereidouni AR, Vahidi B, Mehr TH. The Impact of solid state fault current limiter on power network with wind-turbine power generation. IEEE Trans Smart Grid 2013;4(2):1188–96.
[91] Sarmiento HG, R Pampin. An example in controlling short circuit levels in large metropolitan area. In: Proceedings of the IEEE power engineering society general meeting; 2003. p. 589–94.
[92] CIGRE WG A3.10. Fault current limiters report on the activities of CIGRE WG 3.16. CIGRE technical brochure, CIGRE, Paris, France; 2006.
[93] Firouzi M, Gharehpetian GB. Improving fault ride-through capability of fixed-speed wind turbine by using bridge-type fault current limiter. IEEE Trans Energy Convers 2013;28(2):361–9.
[94] Jafari M, Naderi SB, Hagh MT, Abapour M, Hosseini SH. Voltage sag compensation of point of common coupling (PCC) using fault current limiter. IEEE Trans Power Deliver 2011;26(4):2638–46.
[95] Naderi SB, Jafari M. Impact of bridge type fault current limiter on power system. In: Proceedings of the 7th international conference on electrical and electronics engineering, Turkey; 2011. p. 1–4.
[96] Rashid G, Ali MH. A Modified bridge-type fault current limiter for fault ride-through capacity enhancement of fixed speed wind generator. IEEE Trans Energy Convers 2014;29(2):527–34.
[97] Ye L, Lin L. Study of superconducting fault current limiters for system integration of wind farms. IEEE Trans Appl Superconduct 2010;20(3):1233–7.
[98] Heydari H, Moghadasi AH. Optimization scheme in combinatorial UPQC and SFCL using normalized simulated annealing'. IEEE Trans Power Deliver 2011;26(3):1489–98.
[99] Salami Y, Firouzi M. Dynamic performance of wind farms with bridge-type superconducting fault current limiter in distribution grid. In: Proceedings of the 2nd international conference on electric power energy conversion system, UAE; 2011:1–6.
[100] Elshiekh ME, Mansour DA, Azmy AM. Improving fault ride-through capability of DFIG-based wind turbine using superconducting fault current limiter. IEEE Trans Appl Superconduct 2013;23(3):1204–8.
[101] Ye L, Lin L. Study of superconducting fault current limiters for system integration of wind farms. IEEE Trans Appl Superconduct 2010;20(3):1233–7.
[102] Moghadasi AH, Heydari H, Farhadi M. Pareto optimality for the design of SMES solenoid coils verified by magnetic field analysis. IEEE Trans Appl Superconduct 2011;21(1):13–20.
[103] Haque MH. Improvement of first swing stability limit by utilizing full benefit of shunt facts devices. IEEE Trans Power Syst 2004;19(4):1894–902.
[104] Mohan Mathur R, Varma RK. Thyristor-based FACTS controllers for electrical transmission systems. New York: IEEE Press and Wiley; 2002.
[105] Narimani M, Varma RK. Application of static var compensator (SVC) with fuzzy controller for grid integration of wind farm. In: Proceedings of the 23rd Canadian conference on electrical and computer engineering (CCECE); 2010. p. 1–6.
[106] Shun H, Schmall J, Conto J, Adams J, Yang Z. Voltage control challenges on weak grids with high penetration of wind generation: ERCOT experience. In: Proceedings of the power and energy society general meeting; 2012. p. 1–7.

[107] SVC for grid integration of wind power and damping of power oscillations in a 400 kV interconnector. ABB, FACTS, power and productivity for better world [online]. Available: ⟨www.abb.com/FACTS/⟩; 2011.
[108] Lie X, Liangzhong Y, Sasse C. Comparison of using SVC and STATCOM for wind far integration. In: Proceedings of the international conference on power system technology; 2006. p. 1–7.
[109] Molinas M, Suul JA, Undeland T. Low voltage ride through of wind farms with cage generators: STATCOM versus SVC. IEEE Trans Power Electron 2008;23(3):1104–17.
[110] Mahfouz MM, Sayed MA. Static synchronous compensator sizing for enhancement of fault ride-through capability and voltage stabilization of fixed speed wind farms. IET Renew Power Gener 2014;8(1):1–9.
[111] Koessler RJ. Dynamic simulation of static var compensators in distribution systems. IEEE Trans Power Syst 1992;7(3):1285–91.
[112] Saad-Saoud Z, Lisboa M, Ekanayake J, Jenkins N, Strbac G. The application of STATCOMS to wind farms. Proc Inst Electr Eng 1998;145(5):511–6.
[113] Noroozian M, Petersson N, Thorvaldson B, Nilsson BA, Taylor CW. Benefits of SVC and STATCOM for electric utility application. In: Proceedings of the IEEE PES transmission and distribution conference and exposition; 2013. p. 1143–50.
[114] Aten M, Martinez J, Cartwright PJ. Fault recovery of a wind farm with fixed-speed induction generators using a STATCOM. Wind Eng 2005;29(4):231–9.
[115] Gaztanaga H, Etxeberria-Otadui I, Ocnasu D, Bacha S. Real-time analysis of the transient response improvement of fixed-speed wind farms by using a reduced-scale STATCOM prototype. IEEE Trans Power Syst 2007;22(2):658–66.
[116] Muyeen SM, Takahashi R, Murata T, Tamura J, Ali MH. Application of STATCOM/BESS for wind power smoothening and hydrogen generation. Electr Power Syst Res 2009;79(2):365–73.
[117] Suul JA, Molinas M, Undeland T. STATCOM-based indirect torque control of induction machines during voltage recovery after grid faults. IEEE Trans Power Electron 2010;25(5):1240–50.
[118] Hossain MJ, Pota HR, Ramos RA. Robust STATCOM control for the stabilization of fixed-speed wind turbines during low voltages. Renew Energy 2011;36(11):2897–905.
[119] Ramirez D, Martinez S, Blazquez F, Carrero C. Use of STATCOM in wind farms with fixed-speed generators for grid code compliance. Renew Energy 2011;31(1):202–12.
[120] Linyuan Z, Jinjun L, Fangcheng L. Design and implementation of STATCOM combined with series dynamic breaking resistor for low voltage ride-through of wind farms. In: Proceedings of the energy conversion congress and exposition (ECCE); 2010. p. 2501–6.
[121] Hossain MJ, Pota HR, Ugrinovskii V, Ramos RA. Decentralized control to augment LVRT capability of wind generators with STATCOM/ESS. In: Proceedings of the power and energy society general meeting; 2010. p. 1–8.
[122] Hossain MJ, Pota HR, Ramos RA. Improved low-voltage-ride-through capability of fixed speed wind turbines using decentralized control of STATCOM with energy storage system. IET Gener Transm Distrib 2012;6(8):719–30.
[123] Hossain MJ, Pota HR, Ramos RA. Simultaneous STATCOM and pitch angle control for improved LVRT capability of fixed-speed wind turbines. IEEE Trans Sustain Energy 2010;1(3):142–51.
[124] Bradshaw D. Super reactive power for the power system through superVAR High temperature superconductor dynamic synchronous condensers. In: Presented at the IEEE power engineering society meeting, Denver, CO; June 2004.
[125] Kalsi SS. On grid performance of a superconductor dynamic synchronous condenser. In: Presented at the CIGRE 2005 symposium on power systems with dispersed generation, Athens, Greece; 14–17 April 2005.
[126] Ross M, Kalsi S. Applications of superconducting synchronous condensers in wind power integration. In: Proceedings of the transmission and distribution conference and exhibition, IEEE PES; 2006. p. 272–7.
[127] Teleke S, Abdulahovic T, Thiringer T, Svensson J. Dynamic Performance Comparison of Synchronous Condenser and SVC. IEEE Trans Power Deliver 2008;23(3):1606–12.
[128] Jayanti NG, Basu M, Conlon MF, Gaughan K. Rating requirements of the unified power quality conditioner to integrate the fixed speed induction generator-type wind generation to the grid. IET Renew Power Gener 2009;3(2):133–43.
[129] Moghadasi AH, Islam A, Amini M. LVRT capability assessment of FSIG-based wind turbine utilizing UPQC and SFCL. In: Proceedings of the PES general meeting conference & exposition, IEEE PES; 2014. p. 1–5.
[130] Moghadasi A, Islam A. Enhancing LVRT capability of FSIG wind turbine using current source UPQC based on resistive SFCL. In: Proceedings of the T&D conference and exposition, IEEE PES; 2014. p. 1–5.
[131] Moghadasi AH, Heydari H, Salehifar M. Reduction in VA rating of the unified power quality conditioner with superconducting fault current limiters. In: Proceedings of the power electronic & drive systems & technologies conference (PEDSTC); 2010. p. 382–7.
[132] Po-Hsu H, El Moursi MS, Weidong X, Kirtley JL. Fault ride-through configuration and transient management scheme for self-excited induction generator-based wind turbine. IEEE Trans Sustain Energy 2014;5(1):148–59.
[133] Renewable energy technology: cost analysis series. International Renewable Energy Agency (IRENA); 2010.
[134] Bindeshwar Singh. Introduction to FACTS controllers in wind power farms: a technological review. Int J Renew Energy Res 2012;2(2).
[135] Saravanan M, Slochanal S, Venkatesh MR. P, and J. Application of particle swarm optimization technique for optimal location of FACTS devices considering cost of installation and system load ability. Electr Power Syst Res 2007;77:276–83.
[136] Habur K, Leary DO. FACTS-for cost effective and reliable transmission of electrical energy. Available: ⟨http://www.worldbank.org/html/fpd/em/transmission/facts_siemens.pdf⟩; 2004.
[137] Zhang Y. Techno-economic assessment of voltage sag performance and mitigation [Ph.D. thesis]. University of Manchester; 2008.
[138] Brito M, Cavalcanti M, Limongiu L, Neves F. Low cost dynamic voltage restorer. In: Proceedings of the international conference on renewable energies and power quality (ICREPQ'12), Spain; March 2012.
[139] World Dynamic Voltage Restorer (DVR) Markets. Frost & Sullivan Research Service; 28 Jun 2005.
[140] Gong Wenming, Wang Yun, Hu Shuju, Xu Honghua. A Survey on Recent Low Voltage Ride-Through Solutions of Large Scale Wind Farm. In: Proceedings of the Asia-Pacific Power and Energy Engineering Conference (APPEEC); 2011. p. 1–5.
[141] Fran Li F, Kueck John, Rizy T, King T. A preliminary analysis of the economics of using distributed energy as a source of reactive power supply. Department of Energy (DOE); April 2006. Available at: ⟨http://www.osti.gov/bridge⟩.
[142] Chang H, Lee GH, Sim J, Park K, Oh Sung, Song L, Lee H. Two-stage cryo-cooling design for hybrid superconducting fault current limiter. IEEE Trans Appl Supercond 2010;20(3):2047–50.
[143] Pleva EF, Schwenterly SW, Reis CT. Assembly and test of 5/10MVA HTS transformer. In: Proceedings of the power engineering society general meeting, vol. 2; 2004. p. 1431–5.